water

MDPI

Article

Quaternary Fluvial Terraces as Markers of Climate and Tectonics in the Bradanic Foredeep, Southern Italy

Fabio Olita , Salvatore Ivo Giano *, Mario Bentivenga , Silvia Messina, Marco Piccarreta and Giacomo Prosser

Department of Basic and Applied Sciences, University of Basilicata, Campus Macchia Romana, via Ateneo Lucano 10, I-85100 Potenza, Italy; fabio.olita@unibas.it (F.O.); mario.bentivenga@unibas.it (M.B.); marco.piccarreta@scuola.istruzione.it (M.P.); giacomo.prosser@unibas.it (G.P.)

* Correspondence: ivo.giano@unibas.it

Abstract

Fluvial terraces represent important geomorphological archives for reconstructing the effects of climatic fluctuations, tectonic activity, and base-level changes during Quaternary times. This study investigates the geomorphological and stratigraphic evolution of the Bradano, Basento, and Salandrella River systems within the Bradanic Foredeep of southern Italy, by means of field observations, geomorphological mapping, aerial-photo interpretation, and GIS analyses. Four relative morphostratigrafic orders of Pleistocene fluvial terraces (T_1–T_4) have been identified and correlated across the three drainage basins. No absolute ages are available for these surfaces. The terraced deposits consist of alternating sandy and conglomeratic bodies recording multiple episodes of incision and/or aggradation overlaying erosional surfaces developed on Pre-Quaternary bedrock. Morphometric analyses revealed significant differences in terrace elevation and relative height above the modern channels, among the three investigated basins. The Salandrella basin preserves some of the highest terraced remnants, a pattern compatible with a possible tectonic contribution related to its proximity to the Apennine mountain front. Conversely, the Basento and Bradano basins evidenced a greater influence of lithological conditions, sediment supply, and climate-controlled variations in fluvial dynamics. The results indicate that the evolution of the staircase fluvial terraces reflects the combined influence of glacio-eustatic sea-level fluctuations, Quaternary climatic oscillations, local geological controls, and a possible contribution from regional tectonic deformation. The regional correlation of terraced surfaces highlights the role of the external forcing in shaping landscape evolution, while local differences emphasize the importance of catchment-scale controls within the Bradanic Foredeep.

Keywords: Quaternary geomorphology; fluvial terraces; Bradanic Foredeep; southern Italy

Academic Editor: Achim A. Beylich

Received: 7 July 2026
Revised: 22 August 2026
Accepted: 24 August 2026
Published: 26 August 2026

1. Introduction

Fluvial terraces are relevant geomorphological and stratigraphic archives in the investigation of landscape evolution in Quaternary times. They provide a record of the complex interactions that occurred among climate changes, tectonic uplift, and sea-level variation, furnishing detailed chronological constraints in quantifying water discharge, sediment supplies, and incision rates [1,2]. Consequently, fluvial terrace staircases are widely regarded as one of the most valuable geomorphological archives for unraveling the contribution of climatic and tectonic forcing in the long-term landscape evolution. The stratigraphic architecture and the development of river terrace staircases are globally distributed along the flank of river valleys [1–9]. Their formation is mainly driven by climate changes, which are directly controlled by the relationship between discharge stream and sediment supply [6]. During Pleistocene times, the genesis of fluvial sequences was controlled by cold–warm oscillations. It is widely recognized that cold climate produced an increase in sediment supply, induced by weathering and absence of stable vegetation, thus favoring channel aggradation and thick fluvial deposition [10,11]. Conversely, warm climatic stages trigger a deep vertical incision and decrease the availability of sediments [12,13]. Therefore, palaeoclimatic fluctuations represent the first-order high-frequency driving force for aggradation/incision cycles. However, the geomorphological response of fluvial systems is rarely controlled by climate alone, because climatic fluctuations interact with tectonic uplift, lithological variability and base-level changes, producing different terrace architectures according to the geological setting. In addition to the climate, which controls the timing of depositional and erosional events, the tectonic activity is also important, mainly in the long-term development of fluvial terraces. Regional uplift, working as a main factor, increases the relief energy, thus constraining rivers to incise progressively into the bedrock [14–16]. In this way, the tectonic uplift provides the vertical accommodation space useful for the abandonment, raising and preservation of floodplains at progressively higher elevations [17]. For this reason, distinguishing the relative influence of climatic and tectonic forcing remains one of the main challenges in Quaternary fluvial geomorphology, particularly in tectonically active Mediterranean regions.

Although general conceptual models on relationships between climate and tectonics are well-established for a single-drainage fluvial basin, less information are available on the physical correlation of fluvial terraces pertaining to contiguous hydrographic basins, which still represent a scientific target [17]. Moreover, comparing adjacent drainage basins provides a unique opportunity to distinguish the effects of regional forcing, such as climate and sea-level fluctuations, from those related to local geological and tectonic conditions. Such an approach allows testing for whether terrace development follows a common regional evolutionary pattern or reflects basin-specific controls, thereby improving the understanding of Quaternary landscape evolution in tectonically active regions. This study investigates the geomorphological and stratigraphic evolution of the fluvial terraces preserved within three adjacent drainage basins of the southern Apennines over a fluvial reach of approximately 38 km. The main objectives are to establish a regional morphostratigraphic terrace correlation, reconstruct the relative sequence of incision and aggradation phases, and evaluate the possible influence of climatic variability, tectonic uplift and sea-level fluctuations on the Quaternary evolution of the Bradanic Foredeep. In this context, the preservation of fluvial terraces is strongly controlled by slope processes. Indeed, hillslope inclination acts as a fundamental filter: moderate slopes favor the preservation of the geometric integrity of the deposits, whereas steeper slopes accelerate erosion, leading to the partial or total removal of sedimentary successions. The approach integrates field surveys and interpretation of aerial photos, all incorporated within 5 m resolution digital terrain models (DTMs) in a QGIS application. Beyond establishing a regional terrace correlation, the integrated geomorphological and stratigraphic framework proposed here provides a valuable opportunity to investigate how climatic variability, tectonic uplift and sea-level fluctuations have jointly controlled the evolution of adjacent Mediterranean fluvial systems during the Quaternary. By comparing three contiguous drainage basins developed under similar regional climatic conditions but different local geological settings, this study contributes to distinguishing regional from local controls on terrace evolution. The results provide a regional evolutionary framework for the Bradanic Foredeep and offer new insights into the mechanisms governing the terrace staircase development in

https://doi.org/10.3390/w18172106

tectonically active Mediterranean landscapes. The novelty of this study lies in the integrated comparison of three adjacent drainage basins through a multidisciplinary approach combining detailed geomorphological mapping, stratigraphic analysis and regional terrace correlation. This approach enables a comprehensive reconstruction of the Quaternary landscape evolution of the Bradanic Foredeep and provides a regional framework that may support future investigations in comparable Mediterranean settings.

2. Study Area

The study area is bounded by the eastern front of the southern Apennine chain and the western margin of the Apulian foreland, representing the southernmost and youngest segment of the Bradanic trough [18,19]. The southern Apennines consist of an E-verging fold-and-thrust belt resulting from the convergence of African and Eurasian plates [20–22]. The subduction of the Apulian plate underlying the Apennines, initiated in the lower Pliocene, produced longitudinal movements and activated a compressive regime that later evolved into gravitational sliding toward the depressions [23,24]. This facilitated the formation of structural highs and the remobilization of allochthonous deposits. The belt is composed of several tectonic units derived from different paleogeographic domains that are tectonically overlapped on the buried Apulian platform during the Miocene and until the Pliocene times (Figure 1) [23–26]. The axial zone of the southern Apennine chain forms a mountain ridge up to 2000 m of elevation a.s.l., and a regional catchment drainage divide is NW-SE-oriented, separating the fluvial network toward the Tyrrhenian Sea (south-west), the Adriatic Sea (north-east), and the Ionian Sea (east). The axial zone is composed of Mesozoic to Cenozoic platform carbonate units overthrusted on the coeval deep-sea water pelagic units [18,22]. Miocene flysch and clastic deposits of Pliocene thrust-top basins, both involved in compressive deformation, unconformably lie on these tectonic units. Quaternary tectonics are still active along the axial zone of the chain and produced tectonically induced intermontane basins [27].

The mountain landscape of the southern Apennine axial zone passes eastward to the hilly landscape of the Bradanic Trough. The latter was filled by a Pliocene-to-Pleistocene transgressive–regressive clastic sequence formed of conglomerate, sand, and clay several thousand meters thick [19,23]. The Lower Pleistocene subsidence was responsible for the deposition of marine clay units passing upward to Middle and Late Pleistocene continental deposits constituted by silts, sands, and conglomerates. Volcanic tephra layers coming from the Campanian province and the Vulture volcano are also interbedded in the whole Quaternary clastic succession [28]. The physical landscape of the Bradanic trough is represented by a medium- to low-relief landscape, featured by gently dipping surfaces, less than 3–5° of slope angle, separated by high-angle scarps; both represent the relics of Middle Pleistocene to Holocene staircase marine terraces. The latter terraces are the result of the interplay between Pleistocene tectonic uplift and glacio-eustatic sea-level variations that triggered the vertical incision of the sedimentary top surfaces by the drainage network [29,30]. Number orders and absolute ages of the Ionian marine terraces is still debated, mainly because of the poor and localized condition of outcrops. The terrace numbers range from ten to eleven [31–37]. The development of Ionian hydrographic network is due to a propagation toward east–northeast and southeast, respectively, of the blind-thrusts affecting the eastern segment of the southern Apennines chain. The trellis-type fluvial network of the rivers [29] cuts the marine terraces, producing the progressive entrenchment of rivers in the Bradanic trough deposits. Besides fluvial and marine terraces, one of the most characteristic geomorphological features of the study area is represented by badlands (calanchi), which are extensively developed on the clay-rich deposits of the Bradanic Trough. These landforms occur in their different genetic and evolutionary forms, ranging from incipient rill and gully systems to mature and highly dissected badland landscapes, thus contributing significantly to the distinctive geomorphological setting of the area [38].

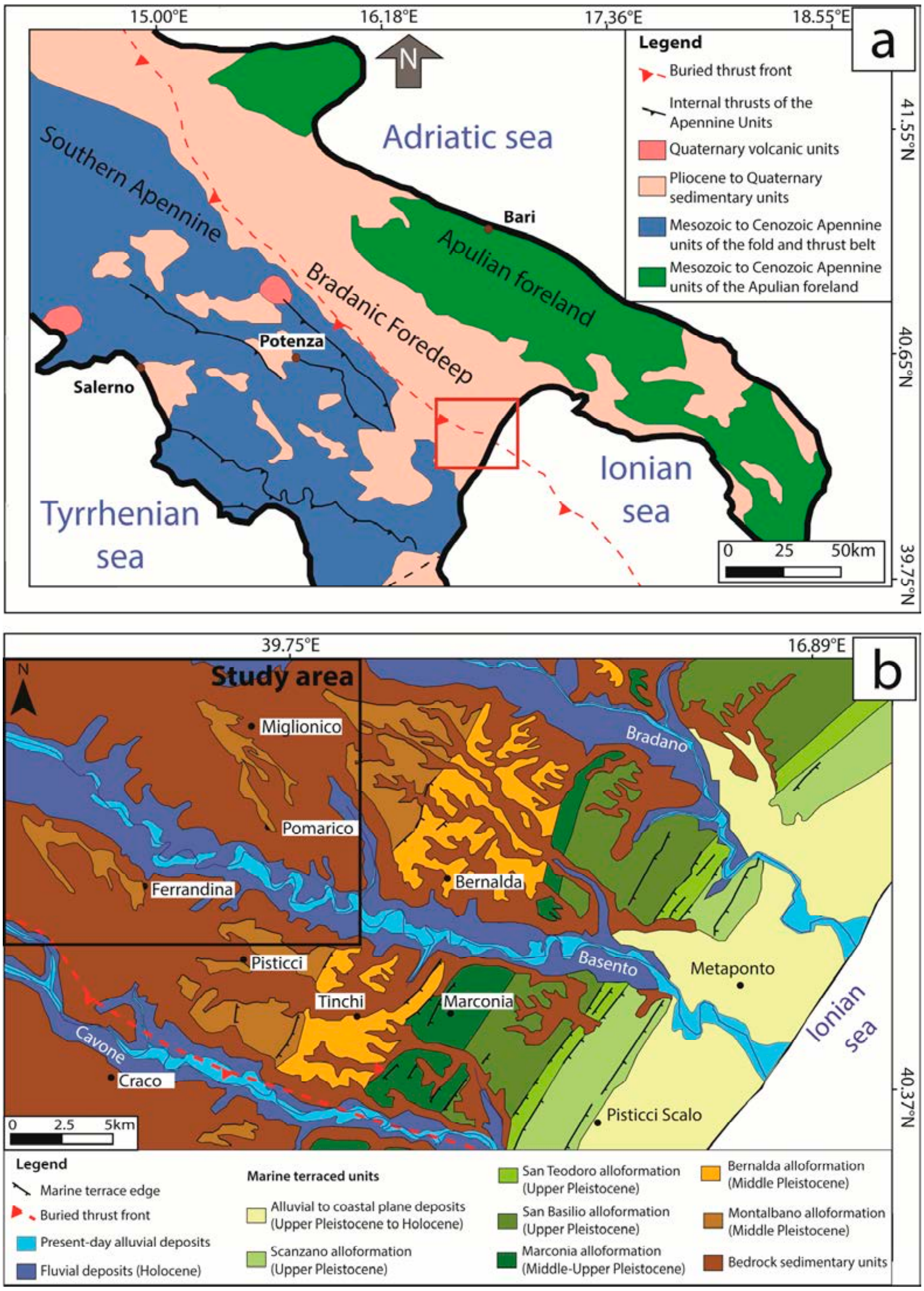

Figure 1. (**a**) Regional geological setting of the southern Apennines and the Bradanic Foredeep; red box indicates the study area. (**b**) Detailed geological map of the study area located between the Bradano and Cavone Rivers, showing the different marine terraced deposits.

The study area partly corresponds to the Metaponto coastal plain, distributed from the Grottole to Pisticci scalo villages including three fluvial sectors of the Bradano, Basento, and Salandrella Rivers (Figure 2). The area crossed by the three above-mentioned rivers corresponds to a large, incised plateau formed by marine terraced deposits; within each catchment fluvial basin, several orders of Pleistocene fluvial terraces are found [16,39–41]. In the three fluvial valleys, the meandering sinuosity of channels increases eastward and attains its maximum value about 3 km before their mouths. Conversely, at the mouth of the three rivers, there is a delta system in which the original cuspidate features are not preserved as a consequence of the Holocene transgression of the Ionian Sea level which deleted the former landforms.

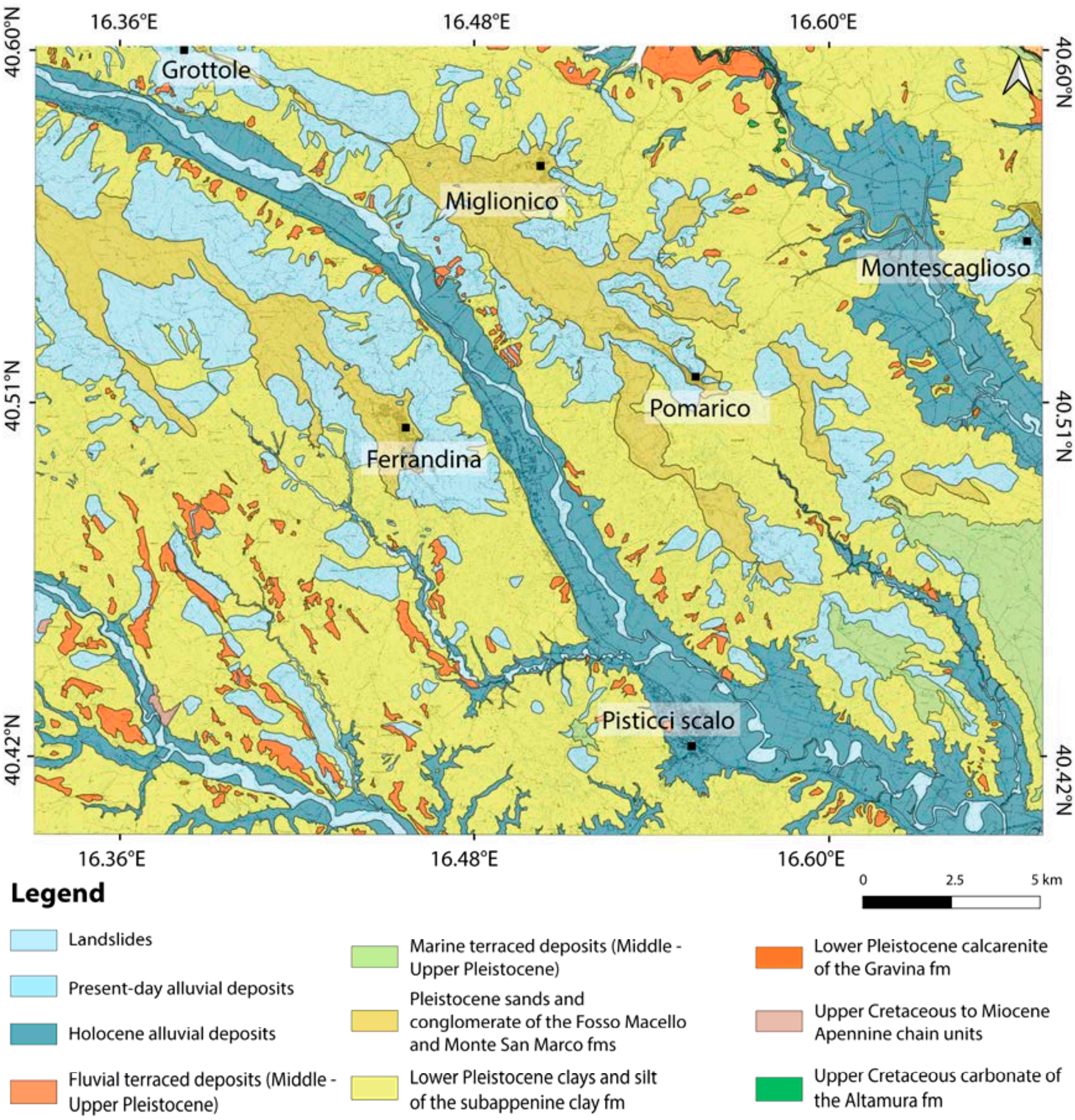

Figure 2. Detailed geological map of the study area showing the distribution of the main lithostratigraphic units and Quaternary deposits.

The climate is Mediterranean, with a mean annual precipitation of about 600 mm and extreme events mainly concentrated from November to March and in the summer, as well as a yearly average temperature ranging from 16° to 17.5°, with an average maximum between 24° and 25.5° during the summer and an average minimum between 8° and 9.5° during the winter [42].

3. Materials and Methods

The recognition and mapping of fluvial and marine terraces were primarily carried out through the integrated interpretation of topographic data, aerial photographs, satellite images and a 5 m resolution digital terrain model (DTM), within the framework of a geological survey, covering approximately 650 km^2. The geomorphological dataset presented in this study is an original dataset produced by the authors between 2024 and 2026 through remote-sensing and GIS-based mapping, complemented by field observations at selected accessible sites. Where suitable exposures were available, field observations were used to characterize sedimentary facies, deposit thickness and basal erosional contacts. By contrast, the planimetric extent, terraces treads and edges, and morphostratigraphic relationships were primarily reconstructed from topographic, DTM and remote-sensing data. A broad distinction between Holocene and Pleistocene deposits was based on the available regional stratigraphic literature, whereas the subdivision into T1–T4 adopted in this study was based on relative morphostratigraphic relationships [8]. Because many terrace remnants are poorly exposed or inaccessible, aerial photographs, satellite imagery and DTM-derived morphology provided the main basis for their recognition and spatial correlation. Where stratigraphic exposures were available, fluvial terraces were further classified as fill or strath according to the relationship between the preserved alluvial deposits and the underlying erosional surface [6]. Where the sedimentary body or basal contact was not directly observable, no genetic classification was imposed solely on the basis of remote-sensing data.

A preliminary step involved the analysis of existing geological maps (Cartografia Geologica d'Italia at 1:100,000 scale, sheets 200 'Tricarico' and 201 'Matera'; https://www.isprambiente.gov.it/it, accessed on 22 December 2024). This was complemented by analyses of topographic maps at 1:10,000 and 1:5000 scales (RSDI Geoportale Basilicata, https://rsdi.regione.basilicata.it/, accessed on 22 December 2024), stereoscopic interpretation of aerial photos and satellite images using Google Earth Pro. Terrace mapping [39] was supported by the combined interpretation of topographic elevations, contour-line analysis and a 5 m resolution DTM, which allowed the verification of physical terrace continuity and the correlation of terrace levels between adjacent drainage basins. All data were imported and digitized in the open-source GIS platform QGIS 3.44 LTR "Solothurn" (https://qgis.org/download/, accessed on 22 December 2024). Field observations were acquired using the QField application on Android mobile devices, allowing real-time positioning and the direct digital recording of geomorphological features onto the Regional Technical Map (CTR) of the Basilicata Region at 1:10,000 scale. In QGIS, polygons have been drawn for each fluvial terrace tread, and raster data corresponding to topography and the 5 m resolution DTM have been incorporated. Analysis involved the automatic generation longitudinal and transverse elevation profiles using the qProf plugin in QGIS. Raster DTM data were used to extract the minimum and maximum elevations of each mapped terrace tread and the elevation of the modern channel at the corresponding longitudinal position. These parameters were subsequently used to calculate the representative elevation and relative height of each terrace remnant above the modern channel (Table 1). A graphical representation of the results has been produced using Adobe Illustrator CS6 version. Longitudinal river profile analysis was used as a method to investigate the tectonic and geomorphological controls on fluvial landscape evolution at multiple scales and to characterize spatial variations in channel and terrace geometry following the approaches proposed in previous geomorphological studies [43,44]. The analysis has been based on the assessment of river deviations from a condition of dynamic equilibrium, following the procedures proposed by [45,46]. This approach has been integrated with the incised-valley model of [47], considering that fluvial morphological evolution may respond to the combined influence of tectonic deformation, relative sea-level fluctuations, lithological variability, sediment supply, inherited valley geometry, and depositional dynamics of the coastal plains. Terrace recognition and nomenclature were primarily based on SW-NE-oriented transverse profiles. Seven transverse profiles, categorized as A-G from north to south, have been established to intersect the maximum number of terraces and perpendicularly to the main river channels. Terrace remnants intersected by each transverse profile were assigned a sequential alphanumeric identifier according to their position along the profile oriented from SW to NE. Thus, for each profile, numbering increases progressively towards the NE (e.g., A1 represents the first terrace remnant intersected by profile A from the SW, whereas A7 represents the last remnant intersected towards the NE). The same identifiers are used in Table 1, providing a direct spatial link between the transverse profiles and the corresponding morphometric data. Furthermore, longitudinal profiles (average NW-SE orientation) were constructed to evaluate the relative elevation, lateral continuity and downstream position of the mapped terrace remnants along the river valleys. This procedure enabled us to assign each terrace in a specific order, which has then been plotted back onto the transverse sections to determine the corresponding order within each drainage basin.

Terrace recognition and correlation were primarily based on geomorphological criteria observable from the 5 m resolution DTM, topographic maps, aerial photographs and satellite imagery. The main criteria included the occurrence of a relatively planar or gently inclined tread separated from the active valley floor by a recognizable topographic break in slope, its relative elevation above the modern channel, lateral continuity, and its geometric position along transverse and longitudinal profiles. Field and stratigraphic observations, where available, were used as supporting evidence rather than as a systematic requirement for terrace recognition. Absolute elevation alone was not considered sufficient for morphostratigraphic correlation. Within each drainage basin, terrace-order assignment was based on the combined evaluation of relative height above the modern channel, terrace treads distribution, lateral continuity and position along the transverse and longitudinal profiles. Cross-basin correlations were accepted only where several of these morphometric and geometric relationships were mutually consistent. Surfaces for which these criteria did not provide a sufficiently reliable morphostratigraphic attribution, or which could not be confidently distinguished from erosional or glacis-like landforms, were excluded from the regional correlation and from the systematic morphometric inventory. Because terrace mapping was predominantly based on remote-sensing and topographic information, uncertainty was retained explicitly rather than converted into a separate categorical confidence value. Where preservation or geomorphic relationships did not permit an unambiguous attribution, composite morphostratigraphic assignments (e.g., T_2–T_3) were retained, as described above. Table 1 reports the morphometric parameters systematically available for the terrace remnants retained in the regional correlation, including minimum and maximum tread elevation, representative tread elevation, internal elevation range, modern-channel elevation, relative height above the modern channel, drainage basin and morphostratigraphic order. Basal contact elevation, depositional thickness, lithology and genetic terrace type were not included in the systematic inventory because these parameters could not be consistently determined for all remnants. Where directly constrained by accessible field exposures or reliable stratigraphic information, these observations are described in Section 4 and illustrated in Figures 3–7.

No direct numerical dating was obtained for the fluvial terraces mapped in this study. The T_1–T_4 nomenclature therefore represents a morphostratigraphic ordering rather than a numerical chronological scheme. Published chronological information was used only where an independent local or regional constraint was available. In particular, the Campanian Ignimbrite tephra layer (~39 ka BP) documented by Boenzi et al. [48] at Masseria La Capriola provides a local chronological constraint for comparison with terrace E7, whereas the Monte Finese marine terrace is tentatively correlated with MIS 13–15 on the basis of the regional marine-terrace framework [31–49]. These constraints and their respective levels of uncertainty are summarized in Table 2. The final geomorphological interpretation was based on the agreement between field observations, topographic analyses, DTM-derived morphometric information and remote-sensing data, providing a consistent basis for terrace recognition and regional correlation.

4. Results

4.1. Stratigraphic and Geomorphological Analyses of Fluvial Terraces

The stratigraphic reconstruction of fluvial deposits and the geomorphological analysis of terraced surfaces enabled the identification of a complex system of fluvial terraces distributed across the Bradano, Basento, and Salandrella drainage basins, which are organized into multiple altimetric orders. The integration of longitudinal and transverse profiles within each of the three catchments has revealed four fluvial terraced surfaces within each basin, ranging from approximately from 60 m up to 400 m of elevation a.s.l. This wide altimetric distribution indicates a polycyclic evolution of the fluvial systems rather than a single episode of vertical incision. The highest terraces (T_4) are generally preserved on the sedimentary top of the area and within a few incised sectors, whereas the lower ones (T_3, T_2, and T_1) are widespread along the river valleys (Figure 3). Where stratigraphic exposures were available, the lower terrace orders commonly showed depositional architectures consistent with fill terraces, whereas some higher surfaces displayed characteristics compatible with strath or erosional terraces. However, this genetic distinction could not be systematically established for all mapped remnants because many surfaces lack suitable exposures. The elevation range between the minimum and maximum tread values was therefore treated as a geomorphometric parameter describing the internal topographic variability of each remnant and not as depositional thickness. Both T_1 and T_2 terraces are fill terraces, whose estimated apparent thickness was computed by measuring field-survey outcrops and the differences between minimum and maximum elevations, which generally range between 5 m and 30 m. These values should be treated with caution as many terraces have been partially modified by anthropogenic activity, hindering accurate stratigraphic reconstruction. Furthermore, T_3 and T_4 are strath terraces which are distributed at higher elevation.

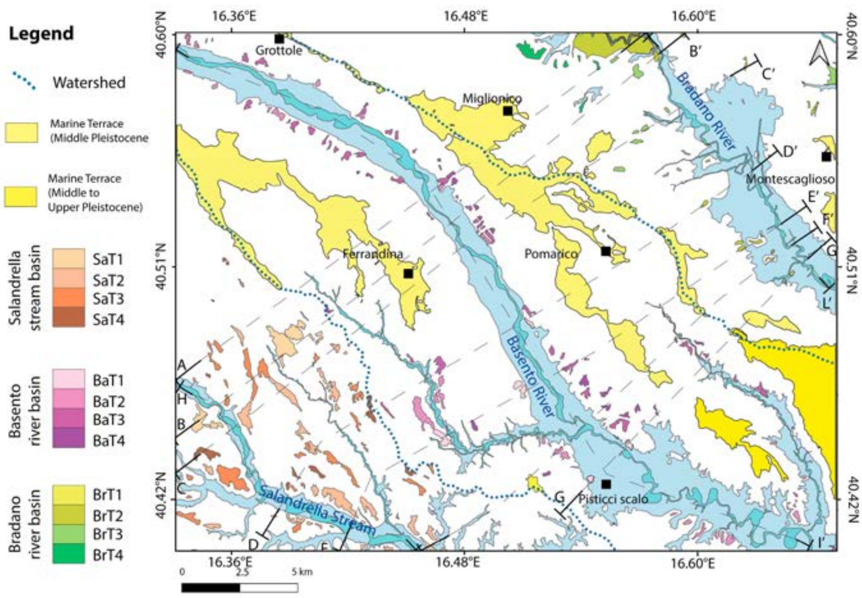

Figure 3. Map of the fluvial terraces detected in the Bradano, Basento and Salandrella catchment basins. The gray dotted lines are the trace of transverse topographic profiles (A-A′, B-B′, etc.) used for the terraces analysis. The river terraces have been organized according to their drainage basin. Monte Finese (M.F.) marine terrace is tentatively correlated with MIS 13–15 (ca. 480–590 ka) and represents an inferred correlation rather than a direct numerical age.

The stratigraphic analysis of the fluvial terraced-deposit outcropping in the Salandrella, Basento, and Bradano fluvial systems highlights significant variability in lithofacies and depositional architecture, consistent with field observations and stratigraphic sections (Figures 4–7). Where stratigraphic exposures were available, the terrace deposits commonly showed multilayer successions characterized by alternating sands and conglomerates, separated by major erosional surfaces and second-order internal discontinuities. The deposits mainly consist of fill terraces organized into multilayer sequences. They are characterized by alternating sands and conglomerates, separated by main erosional surfaces and second-order internal discontinuities. The depositional architecture reflects a complex fluvial system dominated by repeated episodes of incision and aggradation, controlled by base-level fluctuations and changes in hydrodynamic conditions. Figures 4–7 display the Pleistocene alluvial terraces within the Salandrella, Basento, and Bradano alluvial basins. These terraces are located below the remnants of marine terraces forming the top surface of the area and the watershed divide among the Bradano, Basento, and Salandrella River valleys.

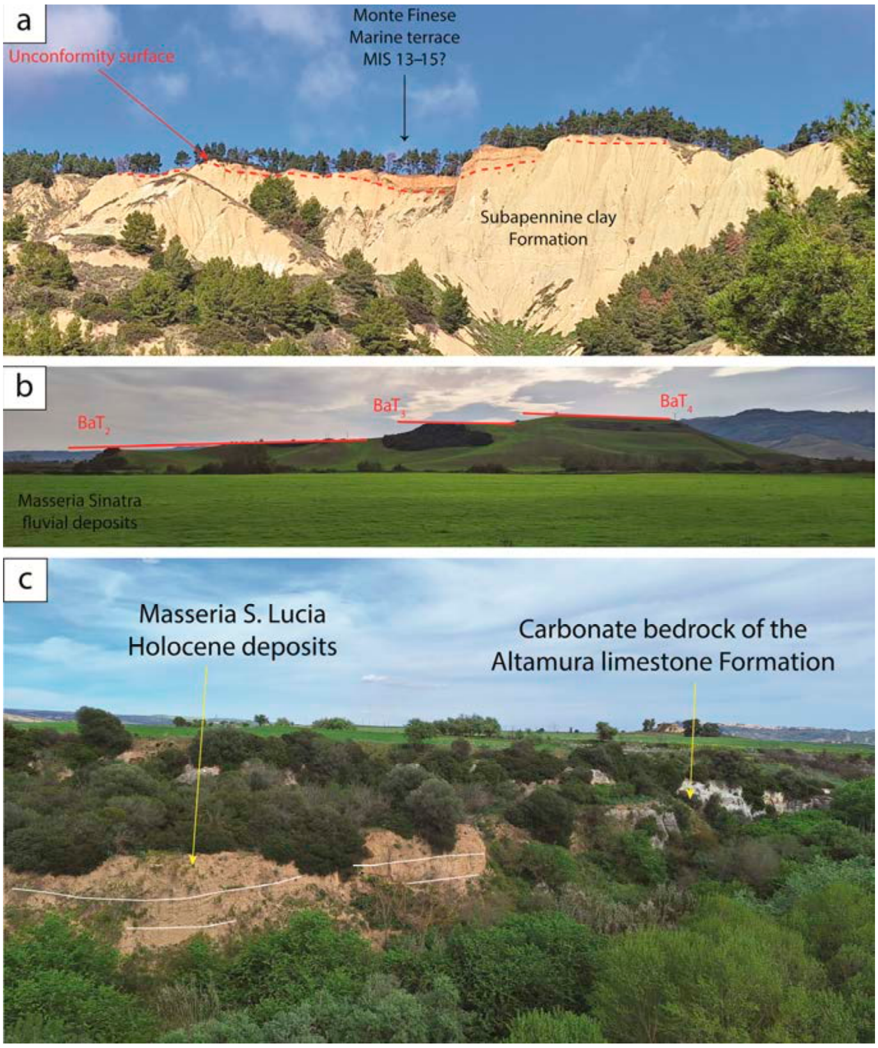

Figure 4. Examples of terraced surfaces and associated deposits of the study area. (**a**) Pleistocene MIS 13-15 marine terrace at Monte Finese, showing the unconformity of the surface (red dashed line) cutting the Subapennine Clays Fm. (**b**) Panoramic view of the BaT_1, BaT_2, and BaT_3 fluvial terraces in the Basento catchment basin (Masseria Sinatra). (**c**) Relationship between the Masseria S. Lucia Holocene deposits and the calcareous substrate of the Altamura Formation in the Bradano fluvial valley, separated by a well-defined erosional surface.

The Middle Pleistocene marine terrace of Monte Finese, located at ~390 m a.s.l., is tentatively correlated with the MIS 13–15 interval (ca. 480–590 ka) on the basis of the regional morphostratigraphic and glacio-eustatic framework proposed for the Ionian marine-terrace sequence [31,32,34,50]. This correlation represents an inferred chronological constraint rather than a direct numerical age of the Monte Finese surface. The four generations of fluvial terraces in all the three fluvial basins are topographically higher than the modern river floodplains containing one/two Holocene terraces which are not considered in the present work. In several instances, the terraces exhibit clearly distinguishable morphologies, subdivided into different orders (Figure 4b). The Holocene terraces consist of sandy deposits with minor conglomeratic beds, resting unconformably on clayey (Salandrella and Basento River valleys) or calcareous (Bradano River valley) bedrocks (Figure 4c). At selected accessible exposures, field observations provided local constraints on the depositional architecture and internal organization of the sedimentary bodies associated with the mapped Pleistocene fluvial terraces. The depositional sequences rest via an angular stratigraphic unconformity upon a predominantly pelitic Pre-Quaternary bedrock, represented by the Subapennine Clays Fm. (Cl). Below, we present the extended sedimentological analysis of the single river basin, according to their relative morphostratigraphic sequence from the geometrically lowest order (T_1) to the highest one (T_4).

4.1.1. Salandrella Stream Basin

In the basin, some areas, such as Serra La Vena (Figure 5a), exhibit more pronounced lateral correlations of the basal surfaces that identify the same terrace order. The SaT_1 terrace represents the geometrically lowest morphostratigraphic unit in the basin. The maximum and minimum elevations of these terraces were identified at Timpa Ottomano (210 m a.s.l.) and Masseria Cocoia (90 m a.s.l.). It consists of predominantly tabular sandy bodies, characterized by high lateral continuity. Structurally, the sands exhibit mainly planar-parallel stratification and, locally, low-angle cross-laminations. This evidence indicates depositional processes governed by subcritical flows under low-flow regime conditions within an active floodplain. Interbedded within the fine-grained deposits and laterally discontinuous, there are conglomeratic lenses, characterized by gravels supported by a sandy matrix (Cg+Sd). These textures are interpreted as the product of high-energy, impulsive hydraulic events attributable to hyperconcentrated flows. Overall, the reduced thickness of the succession and the dominance of fine-grained lithofacies indicate a low-kinetic-energy fluvial system, characterized by frequent hydrodynamic reworking and a highly limited accommodation space.

The SaT_2 terrace, whose best exposures are located in the Monte Priato and Masseria Cammarota areas (Figure 5b–d), exhibits marked vertical complexity and a higher degree of stratigraphic organization compared to the lower order. The maximum and minimum elevations of these terraces were identified at Timpa Ottomano (280 m a.s.l.) and Costa Guardiola (130 m a.s.l.). The succession rests on the Subapennine Clays bedrock (Cl) via a regional erosional surface (Figure 5b). Above this unconformity, poorly stratified sands (Sd) occur with metric thicknesses (~1 m), deposited by high-sediment-concentration flows. The middle and upper portions of the succession show the development of sandy bodies, up to 2 m thick, with planar to cross-stratification, testifying to the transition toward lower-energy river bar and floodplain environments. Tabular and laterally continuous conglomeratic horizons (Cg) are interstratified within the sands, occasionally resting directly on the clayey substrate (Figure 5b,c). At Masseria Cammarota, the depositional architecture highlights a distinct cyclicity between coarse-grained deposits and fine-grained fractions, recording alternating phases of linear incision, coarse bedload transport, and subsequent fine-grained aggradation. Complex stratification and depositional geometries typical of high-energy alluvial environments are observed (Figure 5e).

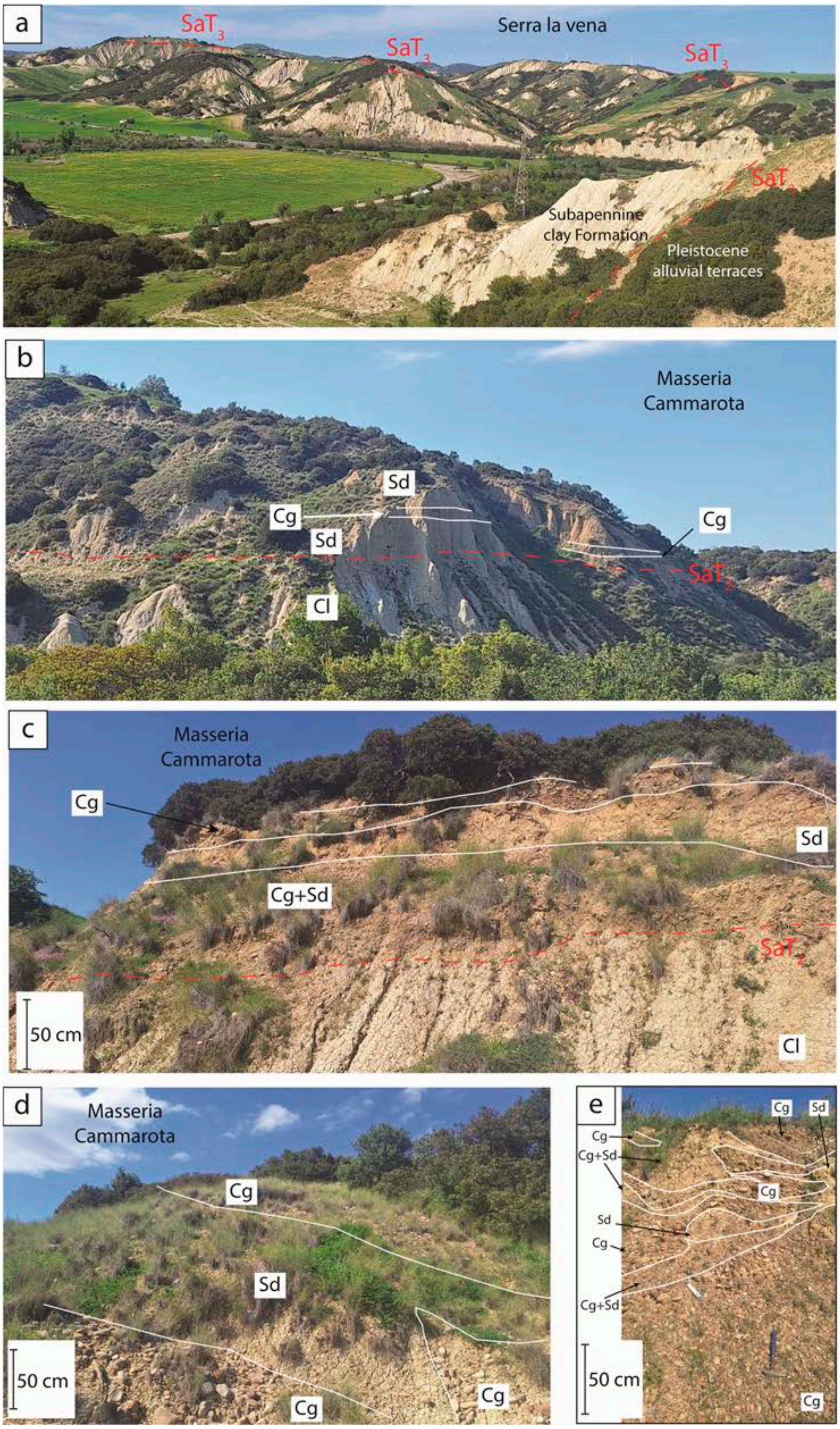

Figure 5. Geomorphological and sedimentological features of Pleistocene terraces in the Salandrella River basin in Monte Priato area. (**a**) Panoramic view of terraced surfaces (SaT3) developed on the Subapennine Clays Fm. (**b**) Overview of the SaT2 sedimentary body showing conglomerates (Cg) and sands (Sd) resting on the Subapennine Clays (Cl). (**c**) Conglomerate in a sandy matrix base and

tabular bedding of alternating sands and conglomerates. (**d**) Details of fluvial lithology associations within the SaT2 deposits in the Masseria Cammarota area, showing alternations of coarse-grained and sand deposits. (**e**) Complex stratification with depositional geometries typical of alluvial environments. White lines mark the boundaries of the main sedimentary bodies. Photos made by F. Olita, April 2026.

The SaT_3 terrace is preserved at higher topographic elevations along the slopes of Monte Priato (Figure 5a) and represents the depositional unit with the greatest sedimentological complexity in the basin. The maximum and minimum elevations of these terraces were identified at Serra La Vena (290 m a.s.l.) and Masseria Caputi (160 m a.s.l.). The lower boundary coincides with a sharp erosional surface that deeply incises the clayey substrate, obliterating the morphology of an ancient incised-valley system. The basal portion of the succession consists of stratified sands (1–2 m thick) deposited in low-energy channels or proximal floodplain environments. This interval is capped by a clast-supported conglomeratic body (0.5–2 m thick) with markedly imbricated clasts, indicative of unidirectional transport as bedload within stable, high-hydraulic-energy channels. Upward, the succession evolves into a thick sandy body (2–7 m) characterized by lenticular geometries of bar and floodplain environments, within which minor, secondary conglomeratic lenses (<1 m) develop, linked to local channel reactivation events. The uppermost section shifts toward reddish sands (2–4 m thick) whose chromatic signature attests to intense oxidizing conditions and prolonged subaerial exposure, related to a depositional stasis or a drastic decrease in the sediment supply rate. Residual sandy–gravelly deposits and discontinuous conglomeratic lenses seal the succession at the top.

The SaT4 terrace represents the oldest Pleistocene unit. It occurs exclusively as isolated, highly dissected remnants along the interfluve summits. The maximum and minimum elevations of these terraces were identified at Masseria Micci (300 m a.s.l.) and Timpa Rocca Vecchia (160 m a.s.l.). The deposit exhibits reduced thicknesses and a poorly expressed internal organization, characterized by an irregular alternation of sands and gravelly horizons. At the base, a continuous conglomeratic layer is almost always identifiable, interpreted as a residual channel lag deposit associated with the initial linear incision phase of the basin. The weak stratification of the overlying deposits suggests a limited sediment budget and unstable hydrodynamic conditions within a fluvial system operating close to a state of geomorphological quasi-equilibrium.

4.1.2. Basento River Basin

In the Basento River basin, the deposits associated with the BaT_1 terrace (Figure 6a,b) exhibit stratigraphic features consistent with the regional trend. The maximum and minimum elevations of these terraces were identified at Macchia (70 m a.s.l.) and Cozzo Serra Cavallo (30 m a.s.l.). The unit is dominated by tabular sandy bodies with high lateral continuity, characterized by planar stratification and low-angle cross-lamination. These sedimentary structures confirm the persistence of subcritical fluvial dynamics within an active, poorly canalized alluvial plain. The intercalated conglomeratic lenses (Cg+Sd), which feature a predominantly sandy matrix, show marginal volumetric development and are associated with episodic hydraulic peaks of hyperconcentrated flows. The marked dominance of fine-grained granulometric fractions and the thin thicknesses indicate a diffused low-kinetic-energy hydraulic regime and a reduced local accommodation capacity.

The BaT_2 terrace exhibits excellent lateral continuity of its depositional surfaces and a clear vertical organization, which is optimally exposed in the Masseria La Capriola section (Figure 6a,b,d). The maximum and minimum elevations of these terraces were identified at Grottole (160 m a.s.l.) (Figure 6c) and Masseria Nobile (60 m a.s.l.). The truncated lower boundary defines a sharp erosional surface carved into the Subapennine Clays (Cl). Directly above this contact, poorly stratified sands (Sd, ~1 m thick) occur, genetically traceable to sheet-flood processes or high-density confined flows. Upward, well-stratified sandy bodies develop (up to 2 m) with planar and cross-stratified structures that document the transition toward bar and floodplain dynamics. Tabular and laterally continuous conglomeratic levels are repeatedly interstratified with the sandy fractions. In high-local-hydraulic-energy contexts, the succession preserves lenticular geometries and convolute soft-sediment deformation load structures, testifying to rapid sedimentation rates and instability of the hydro-plasticized substrate.

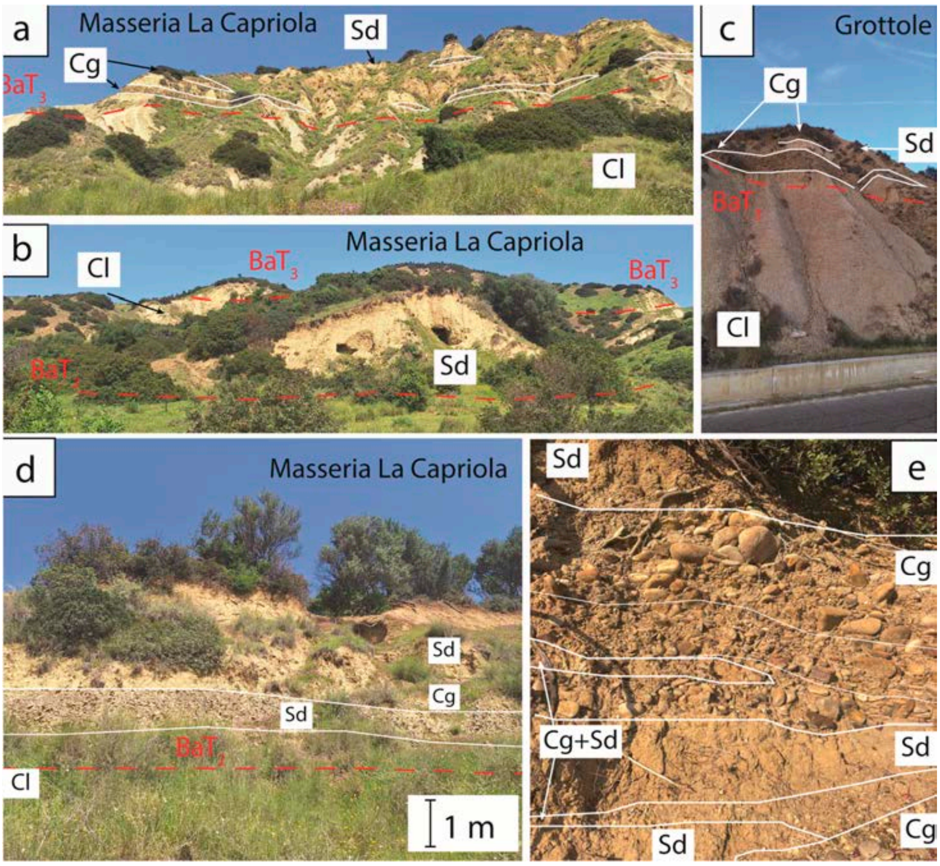

Figure 6. Pleistocene alluvial terraces in the Basento River basin (in Grottole and Masseria La Capriola area). (**a**,**b**) Panoramic views of the Masseria La Capriola area, showing the lateral continuity of erosional surfaces (red dashed lines) and overlying deposits. Outcrops in Grottole (**c**) and in Masseria la Capriola areas (**d**) illustrating the contact between the clayey substrate (Cl) and the basal clastic succession composed of sands (Sd) and conglomeratic lenses (Cg); (**d**) laterally continuous sedimentary conglomerate bodies; (**e**) complex stratification with depositional geometries typical of alluvial environments. White lines mark the boundaries of the main sedimentary bodies. All photos are taken by F. Olita in April 2026 and December 2025.

The BaT_3 terrace finds its best exposures in the middle Basento valley, between Grottole Station and Masseria La Capriola near Pisticci Station (Figure 6), representing the most architecturally complex succession in the region. The maximum and minimum elevations of these terraces were identified at Grottole (260 m a.s.l.) and Masseria La Capriola (100 m a.s.l.). The base is truncated by an extensive, continuous erosional surface that deeply incises the clayey substrate, delineating the morphology of an ancient incised-valley system. The base shows a complex interaction between sandy deposits (Sd, 1–2 m thick) interpreted as low-energy channel fills and clast-supported conglomeratic bodies (0.5–2 m thick) with marked clast imbrication, deposited as bedload under a high-energy regime. The middle section is dominated by a thick sandy body (2–7 m) with well-defined stratification and lenticular geometries, referable to bar and floodplain complexes under subcritical flow regimes. Conglomeratic lenses (up to 1 m thick) document multiple phases of hydraulic reactivation of the system. Toward the top, the succession is characterized by reddish sands (2–4 m) associated with weathering and oxidation processes under conditions of prolonged subaerial exposure and biostasy. Residual sandy–gravelly lithofacies and discontinuous conglomeratic lenses seal the succession.

The BaT_4 terrace shows a slightly higher preservation frequency in the Basento basin compared to the other regional transects, although it is highly fragmented by subsequent erosion. The maximum and minimum elevations of these terraces were identified at Grottole (300 m a.s.l.) and Masseria La Capriola (130 m a.s.l.). The succession has modest thicknesses and consists of a weak alternation of sands and poorly expressed conglomeratic horizons. The basal conglomeratic layer identifies the palaeochannel floor associated with the first phase of Quaternary fluvial incision. The overlying deposits present poor internal organization and limited thicknesses, reflecting a reduced sediment influx within a fluvial system under quasi-equilibrium conditions and low stratigraphic preservation.

4.1.3. Bradano River Basin

In the Bradano basin, the BrT_1 terrace is entirely dominated by a predominantly sandy lithofacies with subordinate and discontinuous conglomeratic lenses (Cg+Sd). The maximum and minimum elevations of these terraces were identified at Masseria Tre Confini Soprano (70 m a.s.l.) and Masseria Salinari (50 m a.s.l.). The sands feature planar stratification and low-angle cross-lamination, indicative of subcritical flows within active alluvial plain environments. The markedly tabular geometric arrangement of the sandy bodies reflects depositional dynamics at low kinetic energy and a confined accommodation space within the valley portion. The discontinuous gravelly lenses record exceptional overbank flooding events or rapidly decelerating hyperconcentrated flows.

The BrT_2 terrace is widely distributed and exposed in the Montescaglioso sectors and near the San Giuliano Lake (Figure 7). The maximum and minimum elevations of these terraces were identified at San Giuliano Lake (110 m a.s.l.) and Iozzo Cantore (80 m a.s.l.). In the Montescaglioso sections, a distinct erosional unconformity carved into the clayey substrate (Cl) bounds the base of the fluvial deposits (Figure 7a). Above this surface, a continuous conglomeratic layer is established, with a thickness varying between 0.7 and 2 m. In the San Giuliano Lake sections, the sharp contact between this lower conglomeratic body (Cg) and the overlying sands (Sd) is clearly observable (Figure 7b). The gravelly lithofacies are clast-supported, consisting of well-rounded elements featuring widespread clast imbrication, interpretable as a channel floor deposit or as longitudinal gravel bars formed under a high-energy flow regime. Above this coarse-grained basal level, the sandy portion develops, within which—in the Montescaglioso successions—altered horizons and palaeosoil levels (Ps) occur, which did not yield conclusive absolute ^{14}C dating (Figure 7c). These markers document significant phases of geomorphological stability of the aggradation surface and intervals of partial or total fluvial inactivity. Overall, the BrT_2 terrace records the transitional alternation between high-energy incisive phases (coarse-grained transport) and subsequent fine-grained depositional phases controlled by a progressively waning hydrodynamic regime.

The BrT_3 terrace exhibits features of high sedimentary complexity analogous to those observed on a regional scale. The maximum and minimum elevations of these terraces were identified at Masseria S. Felice (170 m a.s.l.) and Montescaglioso (100 m a.s.l.). It is defined by a sharp basal contact over a continuous erosional surface cutting through the substrate clays, establishing a palaeo-network of incised channels. The succession begins with stratified sands (1–2 m) deposited in low-energy channel or proximal floodplain environments, followed by a clast-supported and imbricated conglomeratic body (0.5–2 m) associated with high-energy bedload transport. The middle portion is characterized by a thick sandy body (2–7 m) with well-defined stratification and lenticular bar geometries. Secondary lenticular conglomeratic bodies (<1 m) record episodes of local channel reactivation. Toward the top, the appearance of reddish sands (2–4 m) highlights oxidation phenomena linked to prolonged subaerial exposure during phases of depositional stasis. The section terminates with sandy–gravelly deposits and residual conglomerate lenses.

The BrT_4 terrace is preserved exclusively in discontinuous and isolated remnants along the uppermost drainage divides. The maximum and minimum elevations of these terraces were identified at Masseria Grande (190 m a.s.l.) and Masseria Ferito (130 m a.s.l.). The succession features an exiguous thickness and consists of a weak alternation of sands and poorly expressed conglomeratic horizons. At the base, a continuous conglomeratic level is almost always observed, interpreted as a channel floor deposit associated with the earliest stages of linear incision of the basin. The overlying deposits are thin and lack a clear internal organization, reflecting unstable depositional conditions and a reduced detrital input.

The stratigraphic analysis of deposits revealed a well variability of thickness within each single basin and among the terraced surfaces. As illustrated in the geomorphological cross-sections of Figure 8, the spatial distribution of the five older erosional surfaces (eT_1 to eT_5) provides crucial constraints on the multi-phase landscape degradation that preceded and accompanied the deposition of the Pleistocene terrace sequences across the different valleys.

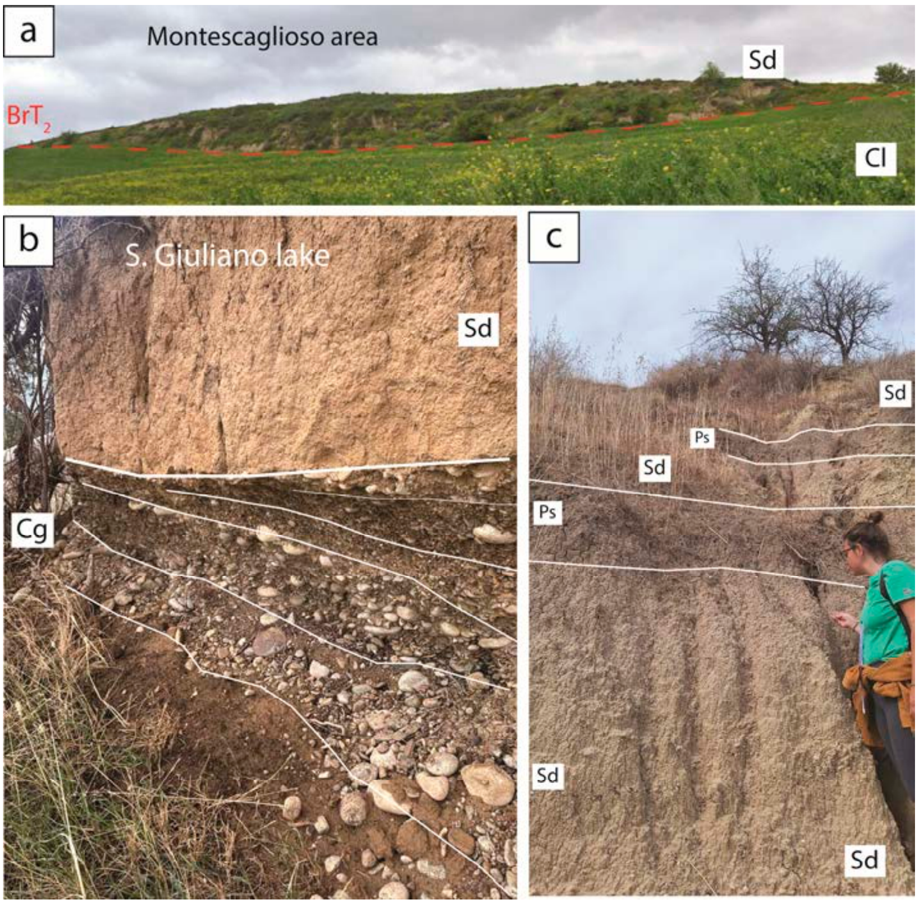

Figure 7. Alluvial successions in the Bradano River basin. (**a**) Panoramic view of Montescaglioso area showing a second-order terrace (BrT_2), the bounding surface between sands (Sd), and the underlying clayey bedrock (Cl). (**b**,**c**) Details of stratigraphic horizons: (**b**) erosional contact between a basal conglomeratic body (Cg) and overlying sands (Sd), with evidence of clast imbrication at Lago di San Giuliano area; (**c**) at Montescaglioso the fluvial terrace shows interbedded palaeosol levels (Ps) within sandy deposits. Photos made by F. Olita in September 2025.

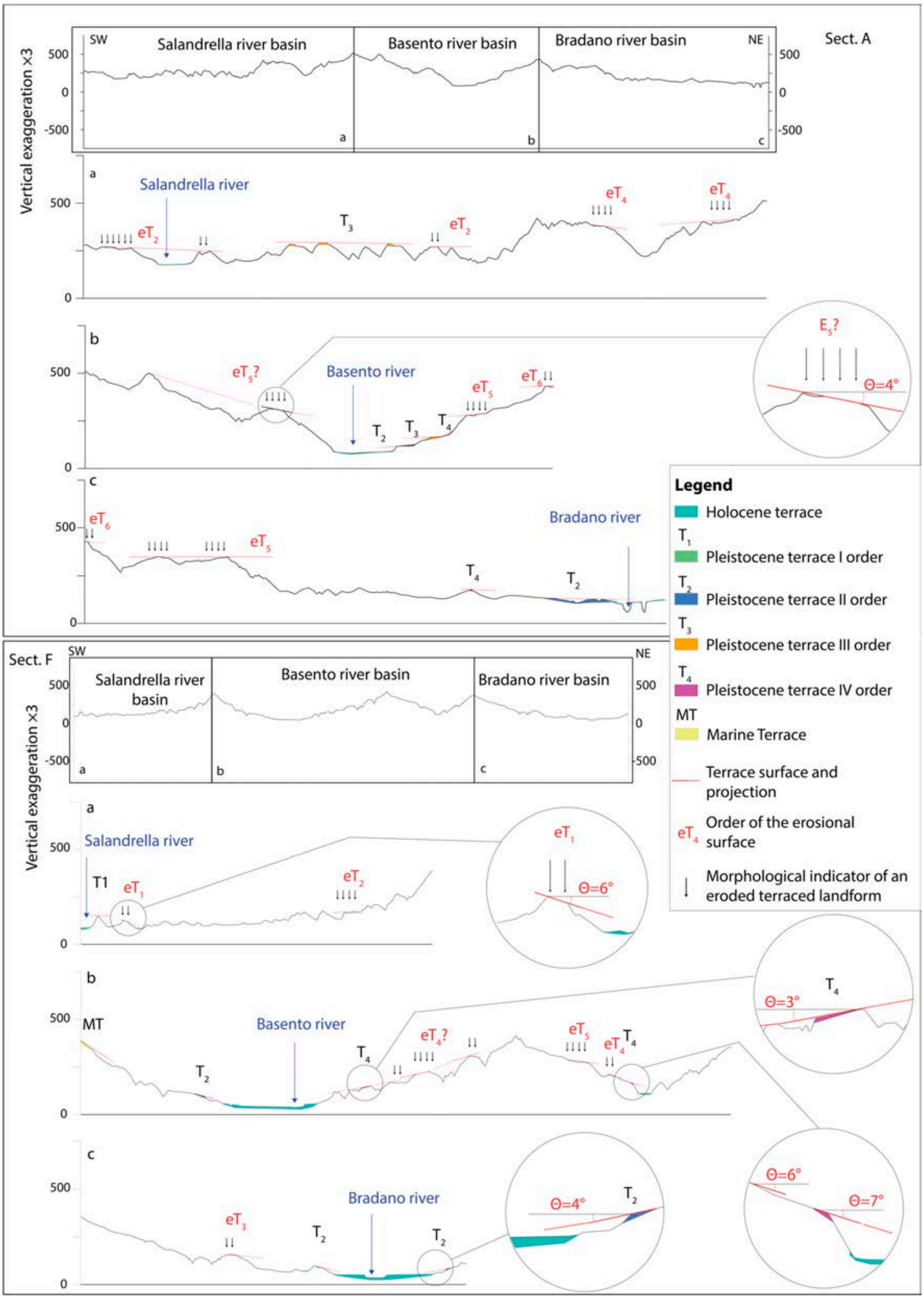

Figure 8. Geomorphological cross-sections (Sect. A and Sect. F) across the Salandrella, Basento, and Bradano River basins. For each section, hillslope profiles are shown with the distribution of erosional surfaces (eT_1 to eT_5) and Pleistocene terrace orders (T_1/T_4). Circular insets provide detailed views of the local geometry and inclination (Θ) of selected terraced surfaces. These angular variations are treated as geomorphological observations and are not interpreted independently as direct evidence of tectonic deformation. Vertical exaggeration is 3× (note: the reported angular values are real and independent of this vertical exaggeration).

Where directly exposed and stratigraphically constrained, terrace deposits show considerable variability in both depositional architecture and thickness among the three drainage basins. For example, the T3 remnants exposed at Serra La Vena display local geometries consistent with strath terraces (Figure 5), whereas T2 terraces documented in the Basento and Bradano basins preserve higher thickness of sedimentary bodies, locally consistent with fill-type terraces (Figures 6 and 7). Some of the better-preserved intermediate terrace successions locally exceed 20 m, whereas other remnants preserve only reduced or discontinuous sedimentary bodies. Because depositional thickness could not be systematically determined for all mapped surfaces, these observations are considered local stratigraphic constraints rather than representative values for each morphostratigraphic order. Overall, the observed variability suggests an important influence of local factors, including basin geometry, sediment availability and preservation conditions.

4.2. Longitudinal Correlation of Fluvial Terraces and Geomorphological Implications

Correlation along longitudinal profiles (Figure 9) integrated with relative height above the modern channel, terrace treads, lateral continuity and position along the transverse profiles allowed morphostratigraphically comparable surfaces to be identified within and across the three basins. Absolute elevation alone was not used as an independent correlation criterion, because terrace elevation varies according to longitudinal position and local valley geometry. The resulting profiles show differences in the geometry and relative elevation of terrace remnants among the three drainage basins, providing the basis for evaluating their regional morphostratigraphic relationships.

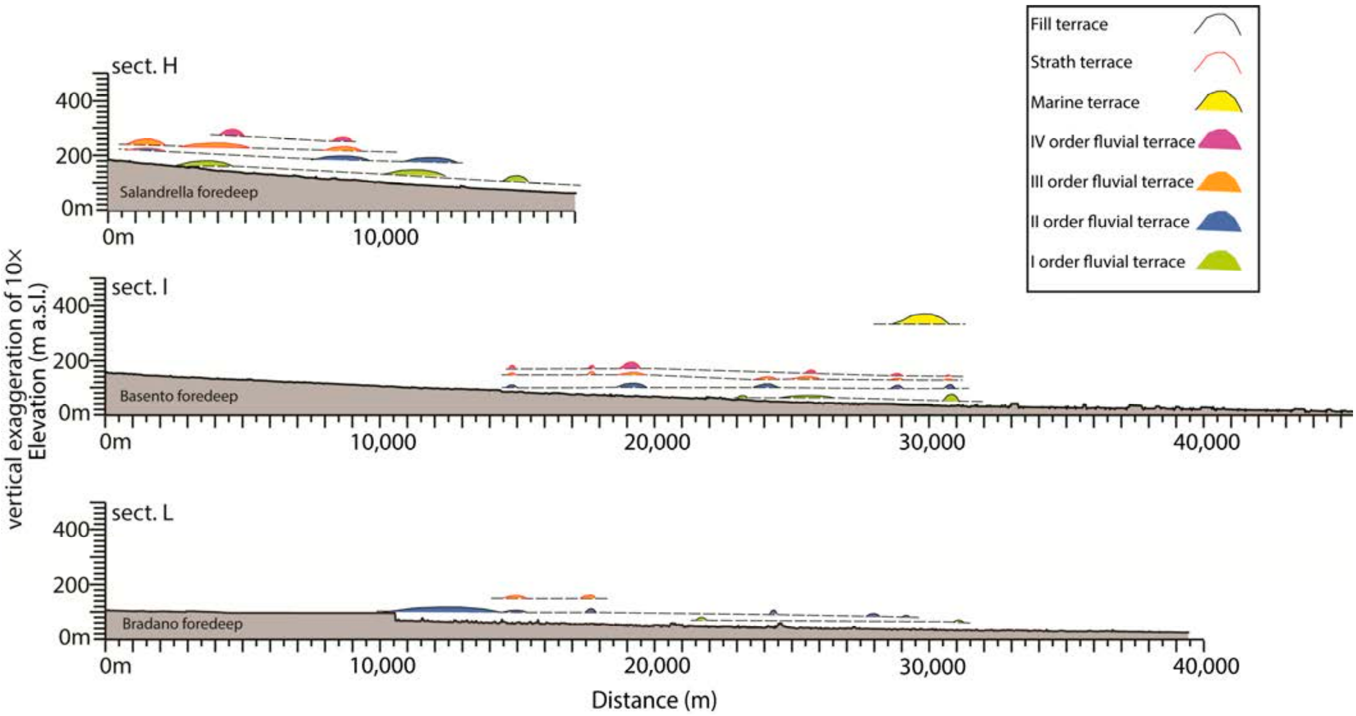

Figure 9. Longitudinal profiles of the Salandrella, Basento, and Bradano Rivers showing the distribution of fluvial terrace orders (from T_1 to T_4) and marine terraces. The legend distinguishes between fill and strath terrace deposits only where the genesis is directly supported by field exposures. Dashed lines represent the morphostratigraphic correlation of terrace remnants along the river profiles and illustrate their relative geometric relationships and longitudinal distribution within the three drainage basins.

The observed morphostratigraphic correspondence suggests that some depositional phases may have developed under broadly comparable regional boundary conditions, potentially including base-level fluctuations and shared climatic forcing [45,46]. However, the lack of direct chronological constraints prevents these correlated surfaces from being considered strictly synchronous.

The combined morphometric and locally available stratigraphic evidence indicate alternating phases of incision and aggradation. Where depositional successions are preserved and directly exposed, their architecture indicates episodes of sediment accumulation probably associated with variations in sediment supply and relative base-level conditions. The altitudinal distribution of terraces and their longitudinal correlation further indicate a regional-scale control on fluvial evolution. This control is consistent with base-level fluctuations and possible contributions from tectonic uplift, in agreement with findings from analogous sectors of the Ionian margin of the southern Apennines [34,48].

The asymmetrical distribution of terrace remnants and their varying relative elevations above the modern valley floors, as illustrated in Figure 10, document marked spatial differences in terrace geometry and valley incision among the three drainage basins. The cross-sections shown in Figure 8 also indicate local variations in the inclination of mapped terrace surfaces. However, terrace elevation and surface inclination may be influenced by several factors, including longitudinal position within the drainage basin, inherited valley geometry, lithological variability, differential preservation and post-depositional modification. The measured terraces' inclination may be compatible with post-depositional tectonic deformation also if they do not independently demonstrate a tectonic tilting. In fact, the tilting was argued based on local faulting activity in the framework of the regional uplift of whole Ionian area [31–41]. The detailed geometric analysis of these cross-sections, particularly through the circular insets in Figure 8, reveals anomalous dip angles (Θ) of the terraced surfaces, confirming that post-depositional crustal deformation locally warped and tilted the Pleistocene deposits, showing a progressive increase in tilt toward the internal mountain sectors.

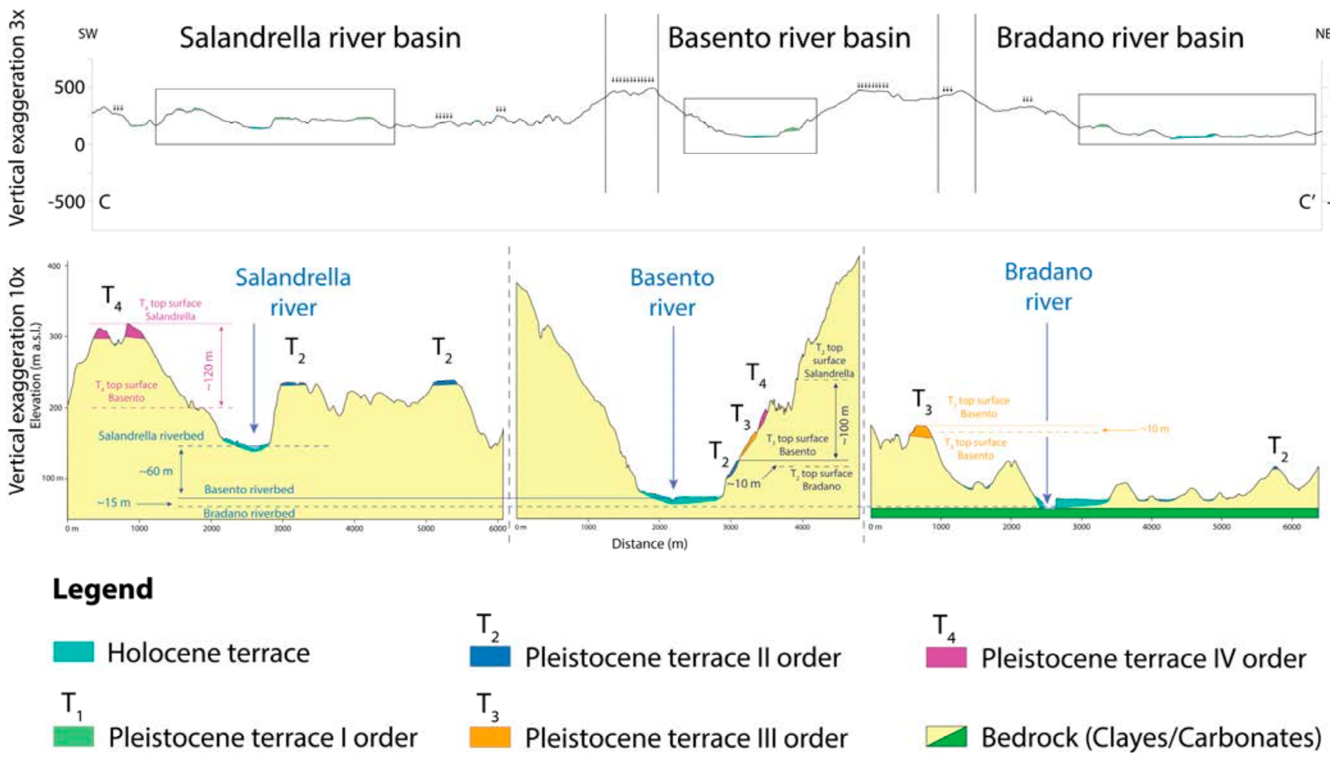

Figure 10. Representative cross-sections of the Salandrella, Basento, and Bradano River valleys. The upper panel displays the regional topographic profile across the three basins, whereas the detailed sections below illustrate the geometry of the terraced sedimentary bodies (Pleistocene to Holocene, orders T1–T4) and their relationship with the geological bedrock (clays/carbonates). The sections

illustrate spatial differences in terrace height relative to the modern valley floors and in terrace preservation among the three drainage basins. Because the compared surfaces occur in different catchments and longitudinal settings, these differences are treated as morphometric observations rather than as direct measures of incision or tectonic uplift.

5. Paleoclimatic Framework of Basilicata During the Last 125 ka

5.1. Approach and Proxy Basis

The palaeoclimatic reconstruction for the last 125 ka in southern Italy is based on the integrated analysis of pollen records, numerical ordination (DCA), independent chronological constraints and geomorphological evidence from fluvial archives.

The pollen data document changes in the relative abundance of temperate and boreal forest taxa, Mediterranean sclerophylls and open-land taxa through time, while DCA axis 1 provides a synthetic gradient that approximates shifts from closed mesic forests to more open and steppe-like vegetation [51–53]. The fluvial record of Basilicata complements the biotic proxies by recording alternations between phases dominated by valley-floor aggradation and phases marked by incision, terrace formation and hillslope stabilization. The chronological control of the palaeoclimatic reference framework is provided by radiometric dating, tephrochronology and well-dated regional records, particularly the varved sequence of Lago Grande di Monticchio and marine records from the central Mediterranean [54–56]. These chronologies constrain the regional climatic framework only and are not used to assign numerical ages to the T_1–T_4 terraces mapped in this study. This framework allows the main pollen-based vegetation shifts and fluvial responses to be linked to North Atlantic–Mediterranean climate variability, including Heinrich events, Dansgaard–Oeschger cycles and the Last Glacial Maximum [52,57,58]. The main trends in vegetation, climatic forcing and fluvial response over the last 125 ka are summarized in Figure 11, which integrates the pollen-based proxies, the DCA axis 1 scores and the reconstructed phases of valley aggradation and incision for the Basilicata catchments.

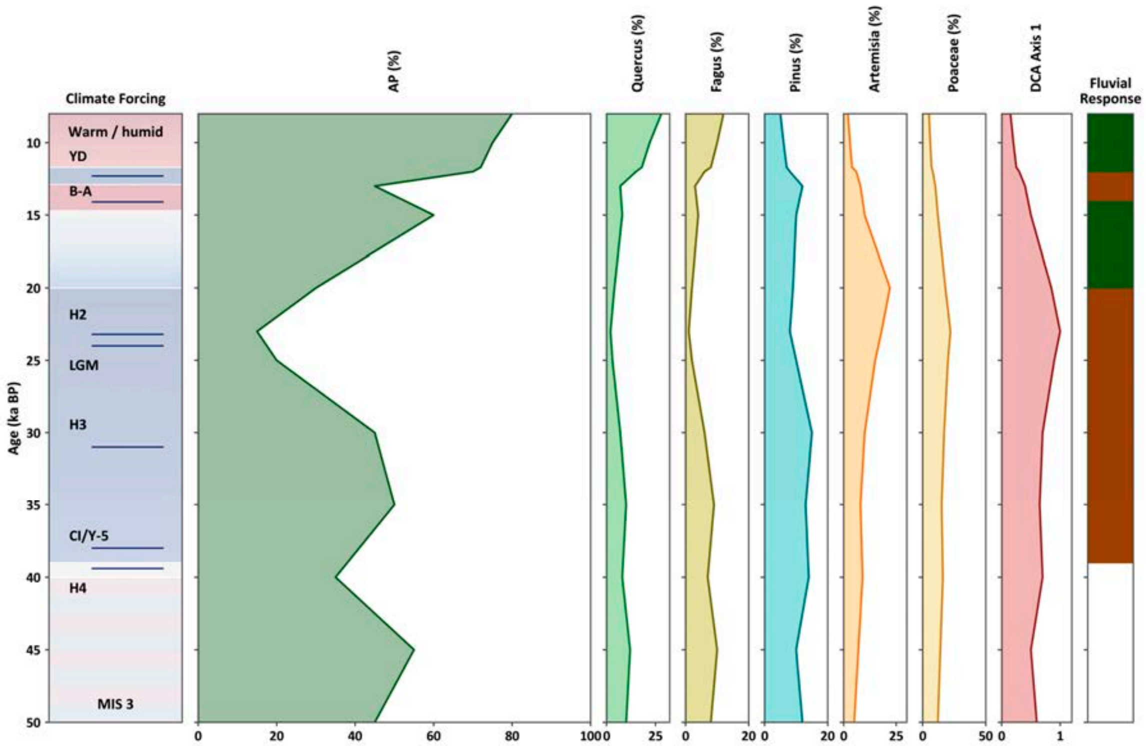

Figure 11. Integrated framework of vegetation, climatic forcing and fluvial response in Basilicata during the last 125 ka. From left to right, the panels show (i) a qualitative climatic forcing column

indicating major warm and cold phases (MIS 5e, MIS 5d–a, MIS 4, MIS 3), the position of Heinrich events and the Last Glacial Maximum; (ii) percentage curves of selected arboreal and non-arboreal pollen taxa and total arboreal pollen (AP); (iii) DCA axis 1 scores summarizing the main gradient from closed temperate–boreal forest to open steppe-like vegetation; and (iv) a schematic subdivision of the fluvial response into phases dominated by valley-floor aggradation (brown) and phases characterized by incision and terrace development (dark green), with a light-green band marking the stable interglacial conditions of MIS 5e (LIG). The age scale is in ka BP and is tied to the chronologies described in Section 5.1.

5.2. 125–115 ka BP (Last Interglacial, MIS 5e)

The earliest part of the reconstruction, between ca. 125 and 115 ka BP, corresponds to the Last Interglacial (MIS 5e). Pollen data from Lago Grande di Monticchio and other southern European records show the dominance of mixed deciduous and evergreen forests, with high abundances of mesophilous taxa and Mediterranean sclerophylls, indicating warm temperatures and relatively humid conditions compared to the subsequent glacial stages [51,54]. DCA scores for this interval are consistent with a closed-forest landscape, with only minor fluctuations towards more open vegetation.

Marine and coastal indicators from the central Mediterranean point to sea-level and hydrological conditions characteristic of an interglacial highstand, in agreement with the pollen-based evidence for dense woodland cover and limited soil erosion [34,36]. In Basilicata, the fluvial archive suggests relatively modest valley-floor aggradation, with rivers maintaining narrow floodplains and limited overbank deposition under stable slopes and well-developed forest cover [48,50].

5.3. 115–50 ka BP (Early Last Glacial, MIS 5d–a and MIS 4)

Between ca. 115 and 50 ka BP, corresponding to the early part of the last glacial cycle (MIS 5d–a and MIS 4), the proxies record a transition from interglacial forested landscapes to progressively more open, cooler and drier environments. Pollen data from Monticchio document repeated forest contractions and expansions linked to stadial–interstadial variability, with several cold phases marked by reduced arboreal pollen and enhanced representation of steppe and shrub taxa [52,55]. These changes are reflected in DCA axis 1 by shifts from the closed-forest endmember towards more open-vegetation scores during stadials and partial reversals during interstadials [52,55]. High-resolution proxy data from Monticchio for MIS 5d–a show that abrupt climate changes during this early glacial interval are associated with variations in sedimentary and geochemical indicators, supporting the interpretation of strong temperature and moisture fluctuations [55]. Marine records from the Ionian Sea and neighboring basins indicate contemporaneous changes in water-mass properties and circulation, consistent with a progressive reorganization of central Mediterranean hydrography during the early glacial [57–59].

In the Basilicata Region, the fluvial response during 115–50 ka BP appears to be characterized by the onset and development of more substantial aggradational phases than during MIS 5e, with thicker valley-floor deposits and more frequent overbank sedimentation. These changes suggest that cooler and more seasonally contrasted climates, together with repeated forest contractions, increased sediment production and delivery to the river systems, while interstadial phases allowed partial stabilization but did not fully restore interglacial conditions [16,48].

5.4. 50–40 ka BP

The oldest part of the record, between ca. 50 and 40 ka BP, corresponds broadly to the earlier part of MIS 3. Pollen data indicate the dominance of mixed temperate–boreal woodland, with relatively high values of mesophilous deciduous taxa and conifers and only limited development of open formations, in agreement with the Monticchio record for this interval [52,55]. The DCA scores are consistent with a generally forested landscape, although punctuated by short-lived shifts towards more open conditions. From a process-based perspective, these cool climatic conditions are compatible with enhanced sediment delivery and aggradational tendencies in regional fluvial systems.

5.5. 40–30 ka BP

Between ca. 40 and 30 ka BP the pollen record documents a clear trend towards more open vegetation, with decreasing forest taxa and expanding steppe and shrub elements, pointing to colder and, on average, drier conditions with enhanced seasonality [52,55]. On this trend are abrupt oscillations that can be related to Heinrich event 4 and associated stadial–interstadial variability seen in the Monticchio and North Atlantic records [54,57]. DCA axis 1 values shift towards the open-vegetation end of the gradient during these phases, in agreement with the reduction in arboreal pollen. Within the regional palaeoenvironmental framework, the progressive reduction in vegetation cover during this interval would have favored increased sediment production and a greater propensity for valley-floor aggradation.

5.6. 30–20 ka BP

The period between ca. 30 and 20 ka BP encompasses the approach to, and culmination of, Last Glacial Maximum conditions. Pollen assemblages are dominated by steppe and herbaceous taxa, with only residual representation of temperate forest elements, indicating a highly open landscape under cold and dry climates [52,55]. Heinrich event 3 and the build-up of LGM conditions coincide with intervals of minimum arboreal pollen and the most extreme DCA scores towards open vegetation [55,57,59]. Fluvial evidence points to sustained and spatially extensive aggradation, with construction of high alluvial fills and widespread valley-floor accumulation, suggesting that sediment supply exceeded the transport capacity of the river systems under reduced vegetation cover, enhanced frost weathering and more frequent high-magnitude runoff events [60]. Marine records from the Ionian Sea and Gulf of Taranto for the same interval show marked changes in water-mass structure, ventilation and productivity, indicating a reorganization of central Mediterranean circulation during Heinrich events and the LGM [54,57,59].

5.7. 20–11.7 ka BP (Last Glacial–Holocene Transition)

From ca. 20 ka BP onwards, the proxies register a progressive, though non-linear, climatic amelioration. Pollen spectra show a gradual increase in arboreal taxa and a decline of steppe elements, pointing to the slow recovery of woodland during deglaciation [52,55]. This trend is interrupted by the Bølling–Allerød interstadial and Younger Dryas cooling, which appear as a phase of enhanced forest development followed by a temporary return to more open vegetation, consistent with other southern European late-glacial records [60]. The fluvial archive mirrors this evolution. Aggradation continues into the early deglacial but is followed by a switch towards incision and terrace formation as discharge regimes change and sediment supply declines. Marine proxies in the Ionian Sea and Gulf of Taranto indicate contemporaneous changes in temperature, salinity and circulation, including the re-establishment of better-ventilated intermediate waters and shifts in surface-water hydrology [57,59].

5.8. From 11.7 ka BP to Present (Holocene Overview)

The Holocene part of the reconstruction is marked by the expansion and subsequent reorganization of temperate and Mediterranean forests. Early Holocene pollen spectra document the rapid spread of mixed deciduous and evergreen woodland under warmer and generally wetter conditions than during the Late Glacial [60–66]. From the mid-Holocene onwards, several records, including Lago Trifoglietti, show a gradual decline of some mesophilous taxa and a relative increase in drought-tolerant Mediterranean elements, indicating increasing seasonality and, at least regionally, a reduction in effective moisture [63]. In fluvial systems, the early to mid-Holocene is characterized by renewed incision and the abandonment of many glacial and late-glacial terraces, reflecting lower sediment yields and more stable slopes under dense forest cover [48]. Later Holocene phases include more localized episodes of renewed aggradation and overbank deposition, often associated with short-lived climatic deteriorations and, in the youngest part of the record, with increasing human impact on catchment vegetation and soil stability [38].

6. Discussion

6.1. Controls on Fluvial Terrace Formation

The sedimentological and stratigraphic architecture of the fluvial terraces in the Salandrella, Basento and Bradano basins indicate that their evolution can be interpreted as resulting from the interplay between climatic forcing, lithological variability, base-level fluctuations and a possible contribution from regional tectonic uplift. This interpretation is consistent with established models of Quaternary fluvial landscape evolution, in which terrace sequences represent a cumulative response to multiple external perturbations [5–9]. Where terraced deposits are directly exposed, the successions display fill-type architectures and locally substantial depositional thicknesses, suggesting that aggradation represented an important component of terrace development. The alternation of sandy and conglomeratic facies, separated by erosional surfaces, records repeated cycles of valley incision and infilling, which may be interpreted as a sedimentary response to Quaternary climatic oscillations. In particular, cold stages are generally associated with increased sediment supply and high-energy fluvial conditions, whereas interglacial stages favor incision and a greater degree of fluvial-profile stabilization [10,11,63].

In the Bradanic foredeep, the base level likely exerted an important control. Proximity to the Ionian margin implies a strong sensitivity to glacio-eustatic sea-level fluctuations, may have modulated incision and aggradation cycles during the Middle to Late Pleistocene evolution of the area [64]. The incision of marine terraces by the drainage network further demonstrates the close coupling between continental dynamics and sea-level changes. Within this broader framework, the morphometric analysis revealed marked spatial variability in the relative height of terrace remnants above the modern channels, as shown in Figure 10. The representative cross-sections in this figure clearly illustrate the asymmetric preservation of terrace remnants and highlight marked differences in relative terrace height (~120 m for T_4 in Salandrella vs. lower values in Bradano), which are here treated as morphometric observations, rather than direct measures of incision or uplift. These differences may reflect the combined influence of base-level changes, longitudinal position of channels, inherited valley geometry, sedimentary dynamics and possible tectonic deformation. The Salandrella basin displays substantially higher elevations than the Basento and Bradano basins, both for Holocene to modern deposits and for Pleistocene terraces. In the representative sections, elevation differences reach 60–75 m relative to adjacent systems for the youngest surfaces and approximately 120 m for terrace T_4. Since the Salandrella and Basento rivers incise broadly similar lithologies, the differences cannot be attributed exclusively to lithological or sedimentary factors.

The observed pattern is compatible with a tectonic contribution. The higher position of the Salandrella system is consistent with its closer proximity to the Apennine front and with the influence of the accretionary prism, which may have contributed to the observed spatial pattern, although the available morphometric data do not allow higher uplift rates to be quantified in this sector. This possible tectonic contribution is also evaluated in relation to the apparent surface inclinations shown in Figure 8; however, the measured dip angles (Θ) are treated as geomorphological observations and not as independent evidence of tectonic tilting. By contrast, the Bradano basin, located towards the Apulian foreland, shows lower relative terrace heights, which cannot by themselves be taken as evidence of relative crustal stability. The spatial differences observed between these domains may therefore be consistent with a differential tectonic influence within the Bradanic foredeep, but they do not provide a direct measure of differential uplift [16–29].

An additional feature is the progressive decrease in elevation differences in the lower morphostratigraphic terrace order, which may reflect changes in several controls through the evolution of the fluvial systems. In the absence of direct chronological constraints, however, this trend cannot be used to infer a temporal attenuation of uplift rates or a Late Pleistocene morphostructural re-equilibration. By contrast, the smaller differences between the Basento and Bradano basins, generally in the range of 10–15 m, may reflect a stronger influence of climatic and sedimentary factors, although a tectonic contribution cannot be excluded. In these systems, the observed differences in terrace position may be related to the presence of carbonate lithologies, which are generally more susceptible to fluvial erosion than the clays of the Subappennine Clays Fm. that characterize the Basento basin. In parallel, the Basento basin is characterized by a larger siliciclastic sediment supply, probably related both to catchment size and to sediment availability, which tends to promote more prolonged aggradational conditions.

A relevant feature is the different elevation between terraces T_2 and T_3 in the two basins. For terrace T_2, the top surface of the Basento system is about 10 m higher than the Bradano, whereas for terrace T_3 the relationship is inverse. This inversion of altitude between older to younger surfaces is difficult to attribute to tectonic uplift alone, because a simple tectonic control would be expected to produce a more spatially coherent pattern. Instead, this pattern suggests a greater sensitivity of the fluvial systems to changes in the balance between water discharge and sediment load, controlled by climatic and lithological factors. In particular, climatic changes may have modulated incision and deposition rates differently in the two basins through successive terrace-forming phases, affecting both transport capacity and sediment availability. It follows that, across successive morphostratigraphic phases, climatic and sedimentary controls may locally overprint a possible tectonic signal [6,64].

No direct numerical ages are available for the fluvial terraces mapped in this study, and the T_1–T_4 nomenclature should therefore be regarded as a relative morphostratigraphic ordering rather than a numerical chronological scheme. Two independent published constraints are considered separately (Table 2). At Masseria La Capriola, the Campanian Ignimbrite tephra (~39 ka BP) documented by Boenzi et al. [48] at the top of a Pleistocene fluvial-terrace succession provides a local chronological reference for comparison with terrace E7, which occurs in the same area. This datum is not transferred as a numerical age to the other T_1–T_4 surfaces. Likewise, the Monte Finese marine terrace is only tentatively correlated with MIS 13–15 (ca. 480–590 ka) according to the regional morphostratigraphic and glacio-eustatic framework [31–50], and this correlation is considered inferred rather than directly dated. Accordingly, the palaeoclimatic framework presented in Section 5 is used to discuss possible regional climatic controls on fluvial behavior but not to assign numerical ages or individual MIS stages to the mapped T_1–T_4 terraces.

6.2. Sedimentary Processes, Morphologic Control and Terraces Arrangement

The sedimentological evidence indicates that the fluvial systems experienced marked temporal variability in depositional style, in response to changes in hydrological conditions and sediment availability. Clast-supported and imbricated conglomeratic facies record high-energy, bedload-dominated conditions typical of high-magnitude flood events, whereas stratified sandy facies reflect lower-energy conditions associated with bar migration and floodplain deposition. The presence of conglomeratic levels within a sandy matrix suggests episodes of hyperconcentrated flows or gravitational processes, consistent with high sediment availability [67]. This depositional variability fits within a broader evolutionary framework in which fluvial systems alternate between high-energy, sediment-rich phases typical of cold climatic conditions and more stable, organized phases during interglacials [10,11,63]. The result is a complex, multistorey stratigraphy, particularly evident in the intermediate terraces. In this context, terrace preservation is also strongly influenced by slope processes. Morphometric analysis shows that, at comparable elevations, terrace remnants occurring on slopes of moderate inclination (Θ = 6.5°) are much better preserved in terms of geometry and sediment-body integrity (Figure 12). By contrast, steeper slopes (Θ = 13.5°) are subject to greater erosion, leading to fragmentation or complete removal of the deposits (Figure 12). This demonstrates that the geomorphic and stratigraphic legibility of terrace sequences depends not only on fluvial processes but also on slope dynamics [10].

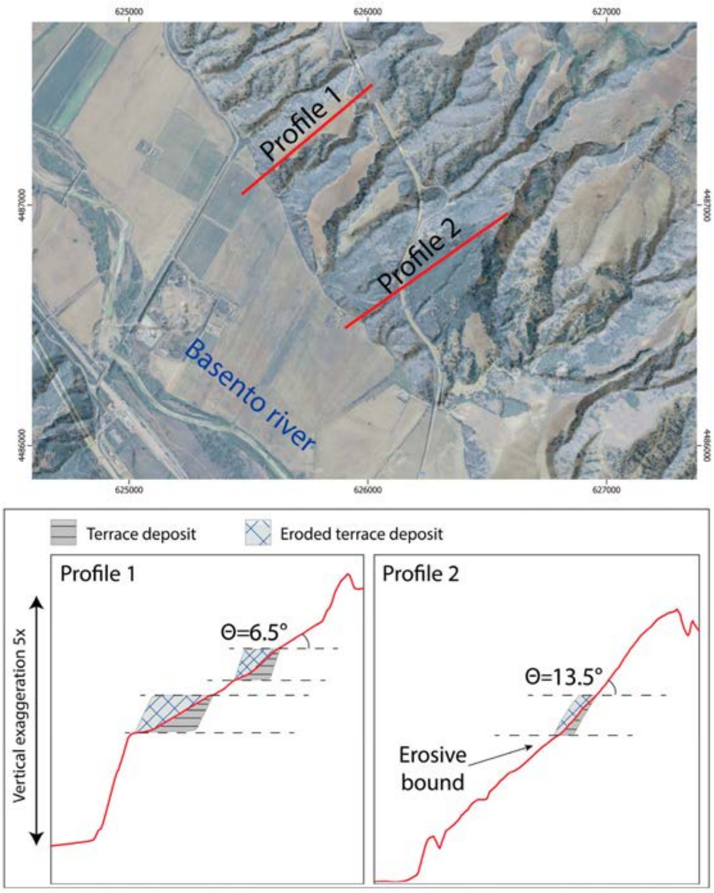

Figure 12. Location of the geomorphological profiles used to assess terrace preservation along the Basento River valley (**top**) and corresponding topographic profiles showing terrace deposits and eroded terrace deposits (**bottom**). The profiles highlight the contrast between terraces preserved on slopes of moderate inclination (Θ = 6.5°) and those eroded on steeper slopes (Θ = 13.5°); vertical exaggeration is 5× (note: the reported slope angle of profiles has vertical exaggeration of 1:1).

The hierarchical distribution of terraces from T_1 to T_4 reflects a polycyclic fluvial evolution controlled by alternating incision and aggradation. The intermediate terraces T_2 and T_3 locally display greater thickness and internal complexity where directly exposed, indicating phases of relative stability during which the system oscillated around dynamic equilibrium conditions. Terrace T_3, in particular, displays a multistorey architecture that records repeated depositional cycles, suggesting a strong interaction between climatic fluctuations and base-level variations. By contrast, terrace T_1 represents the topograhically lowest morphostratigraphic order, characterized by limited sedimentary development and evidence of incision, whereas terrace T_4 appears to be a relict surface, partly deleted by later erosional processes. Correlation among the different basins suggests that some depositional phases may have developed under broadly comparable regional climatic and eustatic conditions, although the lack of direct numerical ages prevents their strict synchronicity from being demonstrated. However, the presence of lateral discontinuities and local differences shows that catchment morphology, lithology and sediment availability modulated the system response, introducing diachronous variability. The fluvial terraces of the Bradanic foredeep constitute an integrated archive of Quaternary evolution, which may record the combined influence of climatic, tectonic and eustatic forcing. The staircase geometry reflects the cumulative response of the system to repeated cycles of incision and aggradation, whereas the spatial differences in relative terrace height and geometry between the basins may be compatible with a differential tectonic influence but do not provide a direct measure of tectonic uplift. Within this overall pattern of progressive incision, the system also exhibits substantial variability, consistent with an important climatic and sedimentary influence on the balance between sediment supply and transport capacity. The resulting picture is that of dynamic fluvial systems, close to unstable equilibrium, in which the observed morphology emerges from the interaction between multiple external forcings and internal self-organizing processes [6,8,63].

7. Conclusions

This study provides a comprehensive geomorphological and stratigraphic reconstruction of the Quaternary evolution of the Bradano, Basento, and Salandrella fluvial systems within the Bradanic Foredeep (southern Italy). The integration of field surveys, geomorphological mapping, DEM analyses, and longitudinal and transverse profile correlations allowed the identification and regional correlation of four relative morphostratigraphic orders of fluvial terraces (T_1–T_4), providing a new regional framework for landscape evolution. The regional correlation of the terrace staircase is consistent with an important influence of Quaternary climatic oscillations and glacio-eustatic sea-level changes on incision and aggradation cycles, whereas systematic variations in terrace elevation and longitudinal river profiles document spatial differences in fluvial and terrace geometry from the Apennine mountain front towards the Apulian foreland. These differences may also be compatible with a contribution from regional tectonic deformation, although they cannot be regarded as direct measures of differential uplift.

The greater stratigraphic complexity of the intermediate terraces (T_2 and T_3) locally suggests that climatic variability, sediment supply and lithological controls locally modulated fluvial responses, together with base-level changes and a possible tectonic contribution. Conversely, the reduced elevation differences observed among the lower morphostratigraphic order (T_1) represent an additional feature of the regional terrace geometry but cannot be used to infer a temporal decrease in uplift rates in the absence of direct chronological constraints. Geomorphological analyses further demonstrate that terrace preservation is strongly influenced by hillslope gradients, with moderate slopes favoring the preservation of terrace geometry and steeper slopes promoting erosion and partial removal of alluvial deposits. Overall, the Bradanic Foredeep preserves an important archive of Quaternary landscape evolution, recording the combined influence of climatic variability, glacio-eustatic forcing, sedimentary dynamics and a possible contribution from regional tectonic deformation. The integrated geomorphological and stratigraphic approach adopted in this study provides a robust framework for investigating Quaternary fluvial evolution in tectonically active Mediterranean regions and highlighting the value of regional terrace correlation for evaluating the relative roles of climatic and tectonic forcing. Future numerical dating of the terrace successions will test and detail the proposed morphostratigraphic correlations and will provide the chronological constraints required to better quantify the relative contribution of the different forcing mechanisms.

Author Contributions: Conceptualization. F.O. and S.I.G.; methodology. S.I.G.; software. F.O.; validation. S.I.G. and F.O.; formal analysis. F.O.; investigation. F.O. and S.M.; resources. G.P.; data curation. F.O. and M.P.; writing—original draft preparation. F.O., M.P. and S.I.G.; writing—review and editing. F.O. and S.I.G.; visualization. F.O. and S.I.G.; supervision. S.I.G. and M.B.; project administration. G.P.; funding acquisition. G.P. All authors have read and agreed to the published version of the manuscript.

Funding: ISPRA, Regione Basilicata, Università della Basilicata joint project on the geological mapping of the 491 Ferrandina sheet (granted to Prof. G Prosser).

Data Availability Statement: The datasets generated and analyzed in this study are not publicly available due to institutional restrictions but are available from the corresponding author upon reasonable request.

Conflicts of Interest: The authors declare no conflicts of interest.

Abbreviations

The following abbreviations are used in this manuscript:

DTM	Digital Terrain Model
DEM	Digital Elevation Model
GIS	Geographic Information System
MIS	Marine Isotope Stage
DCA	Detrended Correspondence Analysis
LGM	Last Glacial Maximum
AP	Arboreal Pollen
NAP	Non-Arboreal Pollen
Fm.	Formation
ka	thousand years ago
a.s.l.	above sea level

Appendix A

Geomorphometric inventory and chronological constraints used for terrace correlation.

Table 1. Geomorphometric inventory of mapped terrace remnants used for morphostratigraphic correlation. Tread and modern-channel elevations were derived from the 5 m resolution DTM. Representative tread elevation is the mid-range of the minimum and maximum tread elevations; Δh is the internal elevation range of each remnant and should not be interpreted as depositional thickness. Terrace IDs refer to the SW–NE transverse profiles A–G; within each profile, numbering increases from SW to NE.

ID	Min–Max Tread Elevation (m a.s.l.)	Mean Tread Elevation (m a.s.l.)	Δh (m)	River Basin	Modern-Channel Elevation (m a.s.l.)	Relative Height Above Modern Channel (m)	Terrace Order	Chronological Constraint from Literature	Suggested Glacio-Eustatic Correlation
A1	268.17–289.6	278.88	21.43	Salandrella	176	102.88	3		2-3a/3b
A2	274–307.94	290.97	33.94	Salandrella	176	114.97	3		2-3a/3b
A3	252.31–306.3	279.31	53.99	Salandrella	176	103.31	3		2-3a/3b
A4	98.7–146.7	122.7	48	Basento	82	40.7	3		2-3a/3b
A5	149.8–190.4	170.1	40.6	Basento	82	88.1	4		3c-3
A6	168.49–181.55	175.02	13.06	Bradano	64	111.02	4		3c-4
A7	94.76–130.46	112.61	35.7	Bradano	64	48.61	2		2
B1	168.34–201.39	184.87	33.05	Salandrella	156	28.87	1		1
B2	228.39–255.62	242	27.23	Salandrella	156	86	3		2-3a/3b
B3	216.55–267.46	242	50.91	Salandrella	156	86	3		2-3a/3b
B4	217.21–271.03	244.12	53.82	Salandrella	156	88.12	3		2-3a/3b
B5	177.52–236.71	207.12	59.19	Salandrella	156	51.12	1		1
B6	164.2–185.82	175.01	21.62	Salandrella	156	19.01	1		1
B7	130.94–156.32	143.63	25.38	Basento	73	70.63	3		2-3a/3b/3c-4
B8	162.54–195.35	178.94	32.81	Basento	73	105.94	4		2-3a/3b/3c-4
B9	150.23–175.22	162.72	24.99	Bradano	73	89.72	3		2-3a/3b
B10	99.42–106.84	103.13	7.42	Bradano	60	43.13	2		2
B11	139.43–156.45	147.94	17.02	Bradano	60	87.94	3		2-3a/3b
C1	289.35–325.25	307.3	35.9	Salandrella	145	162.3	4		3c-4
C2	216.55–267.46	242	50.91	Salandrella	145	97	3		2-3a/3b
C3	217.71–271.03	244.37	53.32	Salandrella	145	99.37	3		2-3a/3b
C4	188.29–213.09	200.69	24.8	Salandrella	145	55.69	3		2-3a/3b
C5	90.67–114.54	102.61	23.87	Basento	68	34.61	2		2-3a/3b/3c-4
C6	115.22–160.29	137.75	45.07	Basento	68	69.75	3		2-3a/3b
C7	177.92–222.38	200.15	44.46	Basento	68	132.15	4		3c-4
C8	157.02–170.92	163.97	13.9	Basento	68	95.97	3		2-3a/3b
C9	159.1–178.52	168.81	19.42	Bradano	55	113.81	3		2-3a/3b

Table 1. *Cont.*

ID	Min–Max Tread Elevation (m a.s.l.)	Mean Tread Elevation (m a.s.l.)	Δh (m)	River Basin	Modern-Channel Elevation (m a.s.l.)	Relative Height Above Modern Channel (m)	Terrace Order	Chronological Constraint from Literature	Suggested Glacio-Eustatic Correlation
C10	108.86–116.44	112.65	7.58	Bradano	55	57.65	2		2
D1	192.05–202.55	197.3	10.5	Salandrella	115	82.3	2		2
D2	190.57–226.19	208.38	35.62	Salandrella	115	93.38	2		2
D3	255.45–282.97	269.21	27.52	Salandrella	115	154.21	3		3a/3b/3c-4
D4	182.67–242.08	212.38	59.41	Salandrella	115	97.38	3		2-3a/3b
D5	161.16–201.35	181.25	40.19	Salandrella	115	66.25	2		2
D6	174.85–205.67	190.26	30.82	Salandrella	115	75.26	3		2-3a/3b
D7	143.68–186.57	165.12	42.89	Basento	54	111.12	3		2
D8	160.62–243.32	201.97	82.7	Basento	54	147.97	2		2-3a/3b
D9	60.04–81.05	70.55	21.01	Basento	54	16.55	1		1
D10	107.19–145.82	126.5	38.63	Bradano	43	83.5	2		2
D11	99.34–103.26	101.3	3.92	Bradano	43	58.3	2		2
E1	133.82–206.32	170.07	72.5	Salandrella	94	76.07	2		2-1
E2	168.56–209.75	189.16	41.19	Salandrella	94	95.16	2		2
E3	183.63–220.48	202.06	36.85	Salandrella	94	108.06	2		2
E4	103.59–148.6	126.09	45.01	Basento	44	82.09	3-2		2-3a/3b
E5	167.7–201.49	184.59	33.79	Basento	44	140.59	4		3c-4
E6	61.03–84.39	72.71	23.36	Basento	44	28.71	1		1
E7	128.46–170.94	149.7	42.48	Basento	44	105.7	3	~39 ka BP (Campanian Ignimbrite tephra; [49])	2-3a/3b
E8	147–162.58	154.79	15.58	Basento	44	110.79	4		3c-4
E9	84.2–125.9	105.05	41.7	Bradano	38	67.05	2		2
E10	97.58–122.01	109.8	24.43	Bradano	38	71.8	2		2
F1	102.6–159.2	130.9	56.6	Salandrella	75	55.9	1		1
F2	335.29–410.01	372.65	74.72	-	-		Marine	MIS 13–15 (ca. 480–590 ka; inferred regional correlation; [31,32,34,50])	13-?
F3	92.26–126.58	109.42	34.32	Basento	39	70.42	3-2		2-3a/3b
F4	133.82–160.34	147.08	26.52	Basento	39	108.08	4		3c-4

Table 1. *Cont.*

ID	Min–Max Tread Elevation (m a.s.l.)	Mean Tread Elevation (m a.s.l.)	Δh (m)	River Basin	Modern-Channel Elevation (m a.s.l.)	Relative Height Above Modern Channel (m)	Terrace Order	Chronological Constraint from Literature	Suggested Glacio-Eustatic Correlation
F5	152.4–171.83	162.12	19.43	Basento	39	123.12	4		3c-4
F6	84.26–99.43	91.84	15.17	Bradano	34	57.84	2		2
F7	80.23–92.71	86.47	12.48	Bradano	34	52.47	2		2
G1	65.65–97.42	81.53	31.77	Basento	36	45.53	1		1
G2	49.4–112.22	80.81	62.82	Basento	36	44.81	2		2-1
G3	110.62–160.47	135.55	49.85	Basento	36	99.55	4		2-3a/3b/3c-4
G4	134.08–159.29	146.69	25.21	Basento	36	110.69	4		3c-4
G5	66.63–70.34	68.48	3.71	Bradano	33	35.48	1		1
X1	68–95	81.5	27	Bradano	33	48.5	1		1

Note: a.s.l. = above sea level. A dash indicates not applicable; blank chronological cells indicate that no independent literature-based chronological constraint was used for that remnant.

Table 2. Chronological constraints used in this study. The suggested constraints provide local or regional reference points and do not represent direct numerical ages of the mapped T1–T4 fluvial terraces.

Chronological Constraint	Site	Material and Dating Method	Age	Stratigraphic Context and Use in This Study	Reference	Uncertainty/Status
Fluvial constraint	Masseria Glionne/Masseria La Capriola, middle Basento River basin	**Material:** Pyroclastic/tephra layer **Dating method:** Tephrochronological correlation	~39 ka BP	**Stratigraphic context:** Tephra layer occurring at the top of the Pleistocene fluvial-terrace succession **Use in this study:** Local chronological constraint for E7; not transferred as a numerical age to the other T1–T4 surfaces	[49]	Published local tephrochronological constraint; not a direct numerical age obtained in this study
Marine constraint	Monte Finese	**Material:** Marine-terrace surface/deposits; no directly dated material **Dating method:** Regional morphostratigraphic and glacio-eustatic correlation	MIS 13–15, ca. 480–590 ka	**Stratigraphic context:** Upper marine-terrace surface at ~390 m a.s.l. **Use in this study:** Upper regional geomorphic reference; not used to directly date the fluvial T1–T4 sequence	[31,32,34,50]	Inferred regional correlation; not directly dated

Note: The Campanian Ignimbrite tephra is used only as a local chronological constraint for comparison with E7. The Monte Finese assignment to MIS 13–15 is an inferred regional morphostratigraphic/glacio-eustatic correlation.

References

1. Gibbard, P.L.; Lewin, J. River incision and terrace formation in the Late Cenozoic of Europe. *Tectonophysics* **2009**, *474*, 41–55. [CrossRef]
2. Bridgland, D.R. The record from British Quaternary river systems within the context of global fluvial archives. *J. Quat. Sci.* **2010**, *25*, 433–446. [CrossRef]
3. Bridgland, D.R.; Keen, D.; Westaway, R. Global correlation of Late Cenozoic fluvial deposits: A synthesis of data from IGCP 449. *Quat. Sci. Rev.* **2007**, *26*, 2694–2700. [CrossRef]
4. Maddy, D.; Bridgland, D.R.; Green, C.P. Crustal uplift in southern England: Evidence from the river terrace records. *Geomorphology* **2000**, *33*, 167–181. [CrossRef]
5. Bull, W.B. *Geomorphic Responses to Climatic Change*; Oxford University Press: Oxford, UK, 1991; p. 326.
6. Bridgland, D.; Westaway, R. Climatically controlled river terrace staircases: A worldwide Quaternary phenomenon. *Geomorphology* **2008**, *98*, 285–315. [CrossRef]
7. Stokes, M.; Cunha, P.P.; Martins, A.A. Techniques for analysing Late Cenozoic river terrace sequences. *Geomorphology* **2012**, *165*, 1–6. [CrossRef]
8. Pazzaglia, F.J.; Brandon, M.T. A fluvial record of long-term steady-state uplift and erosion across the Cascadia forearc high, western Washington State. *Am. J. Sci.* **2001**, *301*, 385–431. [CrossRef]
9. Whitfield, E.; Harvey, A.M. Interaction between the controls on fluvial system development: Tectonics, climate, base level and river capture–Rio Alias, Southeast Spain. *Earth Surf. Processes Landf.* **2012**, *37*, 1387–1397. [CrossRef]
10. Vandenberghe, J. A typology of Pleistocene cold-based rivers. *Quat. Int.* **2001**, *79*, 111–121. [CrossRef]
11. Lewin, J.; Gibbard, P.L. Quaternary river terraces in England: Forms, sediments and processes. *Geomorphology* **2010**, *120*, 293–311. [CrossRef]
12. Antoine, P.; Lozouet, N.L.; Chaussé, C.; Lautridou, J.-P.; Pastre, J.-F.; Auguste, P.; Bahain, J.-J.; Falguères, C.; Galehb, B. Pleistocene fluvial terraces from northern France (Seine, Yonne, Somme): Synthesis, and new results from interglacial deposits. *Quat. Sci. Rev.* **2007**, *26*, 2701–2723. [CrossRef]
13. García, A.F.; Mahan, S.A. The notion of climate-driven strath-terrace production assessed via dissimilar stream-process response to late Quaternary climate. *Geomorphology* **2014**, *214*, 223–244. [CrossRef]
14. Maddy, D.; Bridgland, D.; Westaway, R. Uplift-driven valley incision and climate-controlled river terrace development in the Thames Valley, UK. *Quat. Int.* **2001**, *79*, 23–36. [CrossRef]
15. Westaway, R.; Maddy, D.; Bridgland, D. Flow in the lower continental crust as a mechanism for the Quaternary uplift of south-east England: Constraints from the Thames terrace record. *Quat. Sci. Rev.* **2002**, *21*, 559–603. [CrossRef]
16. Giano, S.I.; Giannandrea, P. Late Pleistocene differential uplift inferred from the analysis of fluvial terraces (Southern Apennines, Italy). *Geomorphology* **2014**, *217*, 89–105. [CrossRef]
17. Cunha, P.P.; Martins, A.A.; Huot, S.; Murray, A.; Raposo, L. Dating the Tejo River lower terraces in the Ródão area (Portugal) to assess the role of tectonics and uplift. *Geomorphology* **2008**, *102*, 43–54. [CrossRef]
18. Pescatore, T.; Renda, P.; Schiattarella, M.; Tramutoli, M. Stratigraphic and structural relationships between Meso-Cenozoic Lagonegro basin and coeval carbonate platforms in southern Apennines, Italy. *Tectonophysics* **1999**, *315*, 269–286. [CrossRef]
19. Tropeano, M.; Sabato, L.; Pieri, P. Filling and cannibalization of a foredeep: The Bradanic Trough, Southern Italy. *Geol. Soc. Lond. Spec. Publ.* **2002**, *191*, 55–79. [CrossRef]
20. Improta, L.; Iannaccone, G.; Capuano, P.; Zollo, A.; Scandone, P. Inferences on the upper crustal structure of Southern Apennines (Italy) from seismic refraction investigations and subsurface data. *Tectonophysics* **2000**, *317*, 273–298. [CrossRef]
21. Mazzoli, S.; Barkham, S.; Cello, G.; Gambini, R.; Mattioni, L.; Shiner, P.; Tondi, E. Reconstruction of continental margin architecture deformed by the contraction of the Lagonegro Basin, southern Apennines, Italy. *J. Geol. Soc.* **2001**, *158*, 309–319. [CrossRef]
22. Patacca, E.; Scandone, P. Geology of the Southern Apennines. *Boll. Soc. Geol. Ital.* **2007**, *7*, 75–119.
23. Casnedi, R.; Crescenti, U.; Tonna, M. Evoluzione dell'avantossa adriatica meridionale nel plio-pleistocene, sulla base di dati di sottosuolo. *Mem. Soc. Geol. Ital.* **1982**, *24*, 243–260.
24. Roure, F.; Casero, P.; Vially, R. Growth processes and melange formation in the southern Apennines accretionary wedge. *Earth Planet. Sci. Lett.* **1991**, *102*, 395–412. [CrossRef]
25. Merlini, S.; Mostardini, F. Appennino centro-meridionale: Sessioni geologiche e proposta di modello strutturale. In *Geologia Dell'italia Centrale*; Congresso Nazionale: Mariano Comense, Italy, 1986; Volume 73, pp. 147–149.
26. Patacca, E.; Scandone, P. Late thrust propagation and sedimentary response in the thrust-belt—Foredeep system of the Southern Apennines (Pliocene-Pleistocene). In *Anatomy of an Orogen: The Apennines and Adjacent Mediterranean Basins*; Springer: Dordrecht, The Netherlands, 2001; pp. 401–440.
27. Di Leo, P.; Giano, S.I.; Gioia, D.; Mattei, M.; Pescatore, E.; Schiattarella, M. Evoluzione morfotettonica quaternaria del bacino intermontano di Sanza (Appennino meridionale). *Alp. Mediterr. Quat. (IL Quat.)* **2009**, *22*, 189–206.

28. Beneduce, P.; Giano, S.I. Osservazioni preliminari sull'assetto morfostrutturale dell'edificio vulcanico del Monte Vulture (Basilicata). *Alp. Mediterr. Quat. (IL Quat.)* **1996**, *9*, 325–330.
29. Gioia, D.; Schiattarella, M.; Giano, S.I. Right-Angle Pattern of Minor Fluvial Networks from the Ionian Terraced Belt, Southern Italy: Passive Structural Control or Foreland Bending? *Geosciences* **2018**, *8*, 331. [CrossRef]
30. Giano, S.I.; Pescatore, E.; Siervo, V. Semi-Automated Extraction and Geomorphic Analysis of Flat Surface Landforms in Large Areas. *Water* **2025**, *17*, 1022. [CrossRef]
31. Brückner, H. *Marine Terrassen in Süditalien. Eine Quartärmorphologische Studie über das Küstentiefland von Metapont*; Düsseldorf Geographische Schriften 14; Selbstverlag des Geographischen Instituts der Universität Düsseldorf: Düsseldorf, Germany, 1980; pp. 1–235.
32. Zander, A.; Fülling, M.A.; Brückner, H.; Mastronuzzi, G. OSL dating of Upper Pleistocene littoral sediments: A contribution to the chronostratigraphy of raised marine terraces bordering the Gulf of Taranto, South Italy. *Geogr. Fis. Din. Quat.* **2006**, *29*, 33–50.
33. Cilumbriello, A.; Tropeano, M.; Sabato, L. The Quaternary terraced marine-deposits of the Metaponto area (Southern Italy) in a sequence-stratigraphic perspective. *Geoacta* **2008**, *1*, 29–54.
34. Caputo, R.; Bianca, M.; D'Onofrio, R. Ionian marine terraces of southern Italy: Insights into the Quaternary tectonic evolution of the area. *Tectonics* **2010**, *29*, TC4005. [CrossRef]
35. Westaway, R.; Bridgland, D. Late Cenozoic uplift of southern Italy deduced from fluvial and marine sediments: Coupling between surface processes and lower-crustal flow. *Quat. Int.* **2007**, *175*, 86–124. [CrossRef]
36. Sauber, D.; Wagner, S.; Brückner, H.; Scarciglia, F.; Mastronuzzi, G. Soil development on marine terraces near Metaponto (Gulf of Taranto, Southern Italy). *Quat. Int.* **2010**, *222*, 48–63. [CrossRef]
37. De Santis, V.; Caldara, M.; Torres, T.; Ortiz, J.E.; Sanchez-Palencia, Y. A review of MIS 7 and MIS 5 terrace deposits along the Gulf of Taranto based on new stratigraphic and chronological data. *Ital. J. Geosci.* **2018**, *137*, 349–368. [CrossRef]
38. Bentivenga, M.; Piccarreta, M. Rapid geomorphological evolution in the Mediterranean Basilicata region (southern Italy) during Little Ice Age. *Catena* **2023**, *231*, 107362. [CrossRef]
39. Nandy, S.; Taloor, A.K.; Chandra Kothyari, G. Mapping of major river terraces and assessment of their characteristics in Upper Pindar River Basin, Uttarakhand: A geospatial approach. *Quat. Sci. Adv.* **2021**, *4*, 100032. [CrossRef]
40. Abbott, J.T. Geomorphology and Geoarchaeology of the Metapontino. *Chora Metaponto* **2011**, *3*, 31–68.
41. Giannandrea, P.; Giano, S.I.; Sulpizio, R. Development of Pleistocene fluvial terraces on the eastern frontal sector of the southern Apennines chain, Italy. *Water* **2019**, *11*, 1345. [CrossRef]
42. Piccarreta, M.; Capolongo, D.; Bentivenga, M.; Pennetta, L. Precipitation and dry-wet cycles influence on badland development in a semi-arid area of Basilicata region (Southern Italy). *Geogr. Fis. E Din. Quat.* **2005**, *VII*, 281–289.
43. Whipple, K.X.; Tucker, G.E. Dynamics of the stream-power river incision model: Implications for height limits of mountain ranges, landscape response timescales, and research needs. *J. Geophys. Res. Solid Earth* **1999**, *104*, 17661–17674. [CrossRef]
44. Kirby, E.; Whipple, K.X. Expression of active tectonics in erosional landscapes. *J. Struct. Geol.* **2012**, *44*, 54–75. [CrossRef]
45. Flint, J.J. Stream gradient as a function of order, magnitude, and discharge. *Water Resour. Res.* **1974**, *10*, 969–973. [CrossRef]
46. Snyder, N.P.; Whipple, K.X.; Tucker, G.E.; Merritts, D.J. Landscape response to tectonic forcing: Digital elevation model analysis of stream profiles in the Mendocino triple junction region, northern California. *Geol. Soc. Am. Bull.* **2000**, *112*, 1250–1263. [CrossRef]
47. Van Wagoner, J.C.; Posamentier, H.W.; Mitchum, R.M.; Vail, P.R.; Sarg, J.F.; Loutit, T.S.; Hardenbol, J. *An Overview of the Fundamentals of Sequence Stratigraphy and Key Definitions*; GeoScienceWorld: McLean, VA, USA, 1988. [CrossRef]
48. Boenzi, F.; Caldara, M.; Capolongo, D.; Dellino, P.; Piccarreta, M.; Simone, O. Late Pleistocene-Holocene landscape evolution in Fossa Bradanica, Basilicata (Southern Italy). *Geomorphology* **2008**, *102*, 297–306. [CrossRef]
49. Abbott, J.T. Late Quaternary Alluviation and Soil Erosion in Southern Italy. Ph.D. Thesis, The University of Texas at Austin, Austin, TX, USA, 1997.
50. Gioia, D.; Bavusi, M.; Di Leo, P.; Giammatteo, T.; Schiattarella, M. Geoarchaeology and geomorphology of the Metaponto area, Ionian coastal belt, Italy. *J. Maps* **2020**, *16*, 117–125. [CrossRef]
51. Watts, W.A.; Allen, J.R.M.; Huntley, B. Vegetation history and palaeoclimate of the last glacial period at Lago Grande di Monticchio, Southern Italy. *Quat. Sci. Rev.* **1996**, *15*, 133–153. [CrossRef]
52. Allen, J.; Brandt, U.; Brauer, A.; Hubberten, H.W.; Huntley, B.; Keller, J.; Kraml, M.; Mackensen, A.; Mingram, J.; Negendank, J.F.W.; et al. Rapid environmental changes in southern Europe during the last glacial period. *Nature* **1999**, *400*, 740–743. [CrossRef]
53. Zumaque, J.; de Vernal, A.; Eynaud, F.; Camuera, J.; Jiménez-Moreno, G.; Combourieu-Nebout, N. High winter precipitation in Southern Europe during the Last Glacial Maximum as inferred from pollen sequences. *Quat. Sci. Rev.* **2026**, *380*, 109906. [CrossRef]
54. Brauer, A.; Allen, J.R.M.; Mingram, J.; Dulski, P.; Wulf, S.; Huntley, B. Evidence for last interglacial chronology and environmental change from Southern Europe. *Proc. Natl. Acad. Sci. USA* **2007**, *104*, 450–455. [CrossRef]

55. Martin-Puertas, C.; Brauer, A.; Wulf, S.; Ott, F.; Lauterbach, S.; Dulski, P. Annual proxy data from Lago Grande di Monticchio (southern Italy) between 76 and 112 ka: New chronological constraints and insights on abrupt climatic oscillations. *Clim. Past* **2014**, *10*, 2099–2114. [CrossRef]
56. Taricco, C.; Ghil, M.; Alessio, S.; Vivaldo, G. Two millennia of climate variability in the Central Mediterranean. *Clim. Past* **2009**, *5*, 171–181. [CrossRef]
57. Casford, J.S.L.; Rohling, E.J.; Abu-Zied, R.; Cooke, S.; Fontanier, C.; Leng, M.; Lykousis, V. Circulation changes and nutrient concentrations in the late Quaternary Aegean Sea: A nonsteady state concept for sapropel formation. *Paleoceanography* **2002**, *17*, 14-1–14-11. [CrossRef]
58. Marino, G.; Rohling, E.J.; Sangiorgi, F.; Hayes, A.; Casford, J.L.; Lotter, A.F.; Kucera, M.; Brinkhuis, H. Early and middle Holocene in the Aegean Sea: Interplay between high and low-latitude climate variability. *Quat. Sci. Rev.* **2009**, *28*, 3246–3262. [CrossRef]
59. Ziemen, F.; Kapsch, M.L.; Klockmann, M.; Mikolajewicz, U. Heinrich events show two-stage climate response in transient glacial simulations. *Clim. Past* **2019**, *15*, 153–168. [CrossRef]
60. Robles, M.; Peyron, O.; Ménot, G.; Brugiapaglia, E.; Wulf, S.; Appelt, O.; Blache, M.; Vannière, B.; Dugerdil, L.; Paura, B.; et al. Climate changes during the Late Glacial in southern Europe: New insights based on pollen and brGDGTs of Lake Matese in Italy. *Clim. Past* **2023**, *19*, 493–515. [CrossRef]
61. de Beaulieu, J.L.; Brugiapaglia, E.; Joannin, S.; Guiter, F.; Zanchetta, G.; Wulf, S.; Peyron, O.; Bernardo, L.; Didier, J.; Stock, A.; et al. Lateglacial–Holocene Abrupt Vegetation Changes at Lago Trifoglietti in Calabria, Southern Italy: The Setting of Ecosystems in a Refugial Zone. *Quat. Sci. Rev.* **2017**, *158*, 44–57. [CrossRef]
62. Joannin, S.; Brugiapaglia, E.; de Beaulieu, J.-L.; Bernardo, L.; Magny, M.; Peyron, O.; Goring, S.; Vannière, B. Pollen-based reconstruction of Holocene vegetation and climate in southern Italy: The case of Lago Trifoglietti. *Clim. Past* **2012**, *8*, 1973–1996. [CrossRef]
63. Vandenberghe, J. River terraces as a response to climatic forcing: Formation processes, sedimentary characteristics and sites for human occupation. *Quat. Int.* **2015**, *370*, 3–11. [CrossRef]
64. Blum, M.D.; Törnqvist, T.E. Fluvial response to climate and sea-level change: A review and look forward. *Sedimentology* **2000**, *47*, 2–48. [CrossRef]
65. Lisiecki, L.E.; Raymo, M.E. A Pliocene-Pleistocene stack of 57 globally distributed benthic $\delta^{18}O$ records. *Paleoceanography* **2005**, *20*, PA1003. [CrossRef]
66. Railsback, L.B.; Gibbard, P.L.; Head, M.J.; Voarintsoa, N.R.G.; Toucanne, S. An optimized scheme of lettered marine isotope substages for the last 1.0 million years, and the climatostratigraphic nature of isotope stages and substages. *Quat. Sci. Rev.* **2015**, *111*, 94–106. [CrossRef]
67. Miall, A.D. *The Geology of Fluvial Deposits*; Springer: Berlin, Germany, 1996; pp. 1–502.